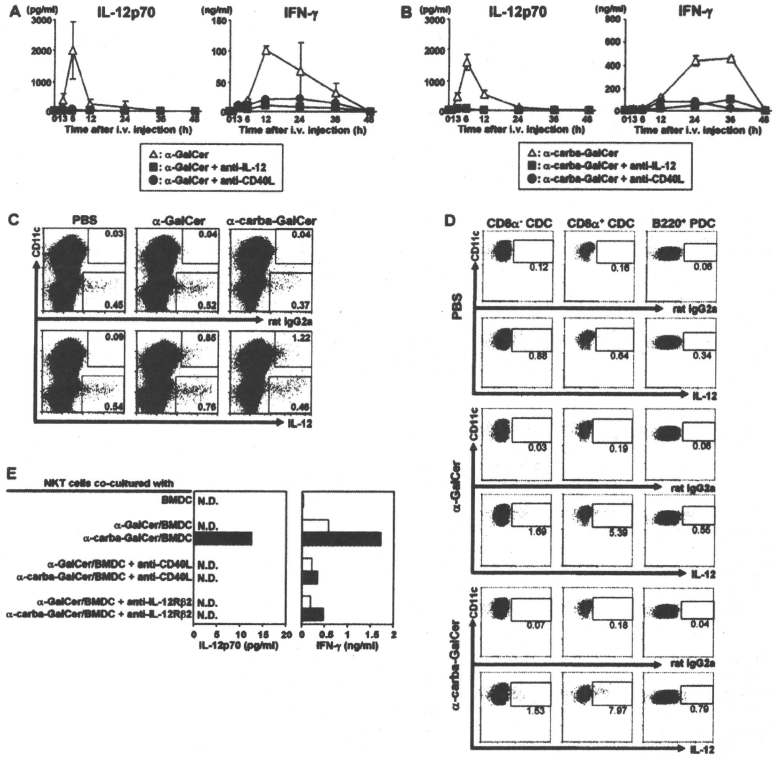

Fig. 3. Mechanisms of α-carba-GalCer-induced IFN-γ production. (A and B) The levels of serum IL-12p70 and IFN-γ after intravenous injection of α-GalCer (2 μg) (A) or α-carba-GalCer (2 μg) (B) were measured by ELISA or the cytometric bead array system at the indicated time points. Indicated antibodies were intraperitoneally injected 24 h before glycolipid injection. Data are means ± SDs from three mice and repeated three times with similar results. (C and D) IL-12p70 production 6 h after intravenous injection of PBS, α-GalCer (2 μg) or α-carba-GalCer (2 μg) by spleen cells (C) and by splenic DC subsets (D). (C) Spleen cells were collected 1 h after glycolipid injection and cultured for 5 h *in vitro*. IL-12p70 production was analyzed by intracellular cytokine staining. (D) CD11c⁺ cells in (C) were further divided into CD8α⁻ CDCs, CD8α⁺ CDCs and B220⁺ PDCs, and IL-12p70 production was analyzed using intracellular cytokine staining. (E) CD40–CD40L interaction and IL-12 dependent production of IFN-γ from NKT cells by α-carba-GalCer-pulsed BMDCs. Glycolipid-loaded or -unloaded BMDCs (2×10^5 cells per 200 μl) were co-cultured with NKT cells (7×10^4 cells per 200 μl) in the presence or absence of indicated mAbs (10 μg ml^{-1}). IL-12p70 and IFN-γ in the supernatant at the indicated time point were measured by cytometric bead array. Results are representative of those from three independent experiments.

Effect on proliferation of human PBMCs by treatment with α-carba-GalCer

We then asked whether α-carba-GalCer induces responses in human Vα24 NKT cells as well as mouse Vα14 NKT cells because α-C-GalCer stimulates mouse NKT cells (20) but not human Vα24 NKT cells (27). We prepared human PBMCs from three healthy volunteers and stimulated the cells with α-GalCer or α-carba-GalCer *in vitro* for 7 days. Contrary to α-C-GalCer, α-carba-GalCer stimulated human Vα24 NKT cells to proliferate in *in vitro* culture better than α-GalCer did (Fig. 6A). It is known that human Vα24 NKT cells can be divided into $CD4^-$ or $CD4^+$ (28). There was no significant

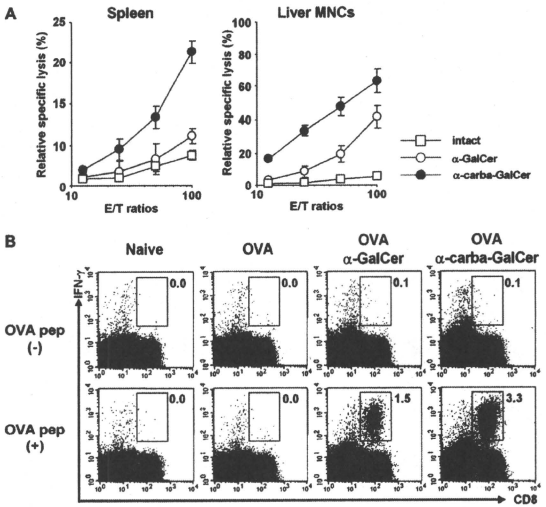

Fig. 4. NKT cell-mediated adjuvant effects on NK and $CD8^+$ T cells induced by α-carba-GalCer treatment. (A) α-carba-GalCer-activated NKT cell-mediated adjuvant effects on NK cell cytotoxicity. Spleen or liver MNCs prepared from B6 mice 4 days previously treated with α-carba-GalCer (closed circles) or α-GalCer (open circles) were used in cytotoxic assays with YAC-1 target cells. Results are representative of those from three independent experiments. (B) Adjuvant effects of α-carba-GalCer-activated NKT cells on the proliferation of IFN-γ producing $CD8^+$ T cells. OVA-loaded *TAP*$^{-/-}$ spleen cells and each glycolipid were injected to B6 mice and 7 days later, IFN-γ production by OVA-specific $CD8^+$ T cells in spleens were analyzed by FACS. Results are representative of those from three independent experiments.

difference in the ratio of $CD4^+$:$CD4^-$ cells after stimulation with either α-GalCer or α-carba-GalCer, indicating that both glycolipids reacted in a similar manner to both $CD4^-$ and $CD4^+$ human NKT cell subsets according to their expansion even though percentage of NKT cells in PBMCs and ratio of $CD4^+$:$CD4^-$ cells in NKT cells were different between individuals (Fig. 6A and B). We also measured cytokine production from human Vα24 NKT cells after stimulation with α-carba-GalCer (Fig. 6C). The α-carba-GalCer-stimulated human Vα24 NKT cells induced all the cytokines tested better than α-GalCer did. Note that significant IL-12 production and IFN-γ production were observed in α-carba-GalCer stimulation rather than α-GalCer, which is in consistent with the results in mice (Figs 2–4).

Discussion

In the present study, we synthesized a new α-GalCer analogue, α-carba-GalCer, by replacing the 5a′-oxygen atom of the pyranose ring of D-galactose (5a′-O) with a methylene group. Despite this minor change on the sugar moiety, α-carba-GalCer, unlike α-GalCer, shows an ability to produce long-lasting T_h1-shifted responses *in vivo*, with significantly larger amounts of IFN-γ, which induces a strong NKT cell-mediated adjuvant activity on NK and $CD8^+$ T cells. The enhanced NKT cell-mediated IFN-γ production and T_h1-shifted cytokine production induced by α-carba-GalCer are due to augmented IL-12 production by DCs via CD40–CD40L interaction between $CD8\alpha^+$ CDCs and NKT cells (Fig. 3B–D); *in vivo* injection of antibodies against CD40L or IL-12 (Fig. 3B) or *in vitro* treatment of antibodies against CD40L or IL-12R (Fig. 3E) inhibit IFN-γ production.

One possible explanation for this enhanced T_h1-shifted cytokine production is likely to be the stable structure of α-carba-GalCer compared with α-GalCer. It has been reported that α-C-GalCer bearing a C-glycosidic (ether) linkage to the ceramide portion exhibited enhanced T_h1-activity in mice (20). Since the ether linkage of α-C-GalCer is stable and would not be degraded by glycosidase, α-C-GalCer is considered more resistant against decomposition than α-GalCer *in vivo*. Thus, it is speculated that an α-C-GalCer–CD1d complex could be maintained for a longer time than α-GalCer, leading to a stable triple complex, and generate enhanced T_h1-biased responses. In fact, NKT cell responses to α-carba-GalCer seem quite similar to those to α-C-GalCer, in terms of T_h1-shifted cytokine production and increased CD40L expression on activated NKT cells.

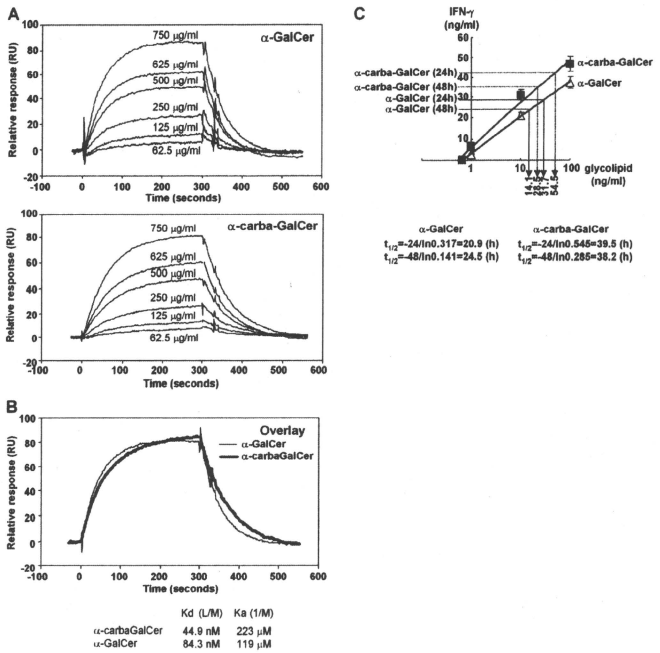

Fig. 5. Binding affinity of soluble invariant Vα14/Vβ8 onto α-carba-GalCer-loaded CD1d. (A) Affinity and kinetics of soluble Vα14/Vβ8 binding to CD1d loaded with α-GalCer (upper panel) or α-carba-GalCer (lower panel). Increasing concentrations from 62.5 μg ml^{-1} to 750 μg ml^{-1} of soluble Vα14/Vβ8 were injected for 5 s over the indicated glycolipid-loaded CD1d. The binding responses of six concentrations are shown superimposed. (B) Alignment of kinetics profile (750 μg ml^{-1}) (A) with α-GalCer and α-carba-GalCer. K_d values (μM) were calculated from equilibrium binding. Kinetic and equilibrium binding values are the mean of at least two independent experiments. (C) Stability of α-GalCer and α-carba-GalCer. The α-GalCer or α-carba-GalCer (100 ng) were incubated for 24 or 48 h with mouse liver microsomes (50 μg) at 37°C. The α-GalCer or α-carba-GalCer was extracted by chloroform and co-cultured with spleen cells (10^5 cells per 100 μl) for 72 h. IFN-γ production in the supernatant was analyzed by cytometric bead array. The metage lines express the amounts of IFN-γ in the culture 72 h after stimulation with known amounts of α-GalCer or α-carba-GalCer. The half lives of glycolipids were calculated from amounts of IFN-γ generated by the assumed concentration of microsome-treated glycolipids. Results are representative of those from three independent experiments.

Similarly to α-C-GalCer, α-carba-GalCer has a stable ether linkage instead of the glycosyl (acetal) bond of α-GalCer, indicating that α-carba-GalCer is resistant to degradation by hydroxylation. This speculation is supported by the data obtained by the liver microsome assay demonstrating that α-GalCer is more susceptible to degradation than α-carba-GalCer is (Fig. 5C). Therefore, α-carba-GalCer could stimulate NKT cells for a longer period than α-GalCer and induce enhanced T_h1 cytokine production.

The second possibility is the more stable high affinity interaction of the NKT TCR with α-carba-GalCer–CD1d complexes (see Fig. 5A and B) than α-GalCer–CD1d complexes. According to the crystal structure of human NKT TCR–CD1d–α-GalCer reported by Borg *et al.* (29), the 5a′-O of α-GalCer does not make a hydrogen bond with any residues in the complex. Additionally, Pro28 at the CDR1 region of the Vα14 TCRα chain is placed at a spatially near position to the 5a′-O of α-GalCer. In the case of α-GalCer, it causes repulsion of the non-polar (hydrophobic) amino acid Pro28 and the hydrophilic 5a′-O. On the other hand, in the case of α-carba-GalCer, the 5a′-O is replaced by a hydrophobic methylene group so that the interaction between the Pro28 and the 5a′-methylene group would be enhanced by the hydrophobic interaction. As a result, the binding of α-carba-GalCer-loaded CD1d to the TCR becomes more stable than that of α-GalCer-loaded CD1d because of a slight increase

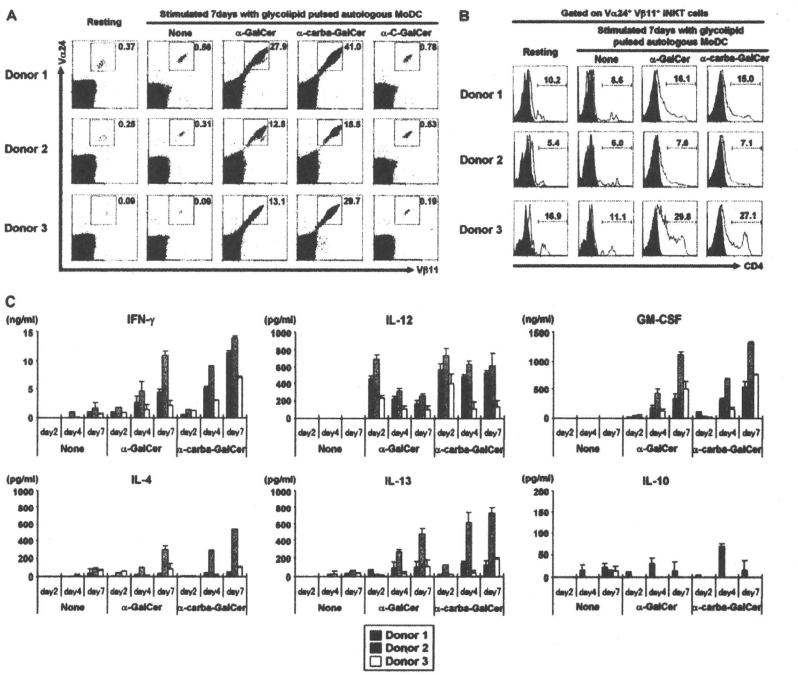

Fig. 6. Proliferation and cytokine production of human Vα24+ NKT cells after stimulation with α-carba-GalCer. (A and B) PBMCs (2×10^5 cells per 200 μl) prepared from healthy volunteers were cultured in the presence or absence of indicated glycolipids (100 ng ml^{-1}) for 7 days. The percentages of Vα24+ Vβ11+ NKT cells (A) and CD4+ cells in Vα24+ Vβ11+ NKT cells (B) were analyzed by FACS. Results are representative of those from three independent experiments. (C) Cytokine levels in the culture supernatants of human PBMCs stimulated with PBS, α-GalCer (100 ng ml^{-1}) or α-carba-GalCer (100 ng ml^{-1}) were measured by the cytometric bead array system at the indicated time points. Data are means ± SDs from three healthy volunteers and were repeated three times with similar results.

in their affinity (Fig. 5A and B). Since Pro28 is conserved in mouse Vα14 and human Vα24 NKT TCRs, human Vα24 NKT cells could also stably bind with the α-carba-GalCer–CD1d in exactly the same way as on mouse NKT cells.

In fact, α-carba-GalCer activates human Vα24 NKT cells from healthy volunteers to proliferate and produce cytokines *in vitro*, whereas α-C-GalCer could not stimulate human NKT cells (Fig. 6). This may be explained by the possibility that the glycosidic oxygen atom (glycosidic-O) bridging between the sugar moiety and the ceramide portion is important for presentation by human CD1d. According to the crystal structure of the complex between the glycolipid and mouse CD1d, the hydrogen bond length between the oxygen atom of Thr156 and glycosidic-O is 3.44 Å (19). Besides, in the crystal structure of the complex between the glycolipid and human α-GalCer, the distance between the oxygen atom of Thr154 and the glycosidic-O is 2.83 Å (9). Therefore, the Thr154 in human CD1d makes a hydrogen bond with glycosidic-O that is shorter and tighter than that with the Thr156 of mouse CD1d. This indicates that the interaction between the human Thr154 and the glycosidic-O is one of the key hydrogen bonds in the complex between α-GalCer and human CD1d for fixing α-GalCer firmly in binding site of human CD1d. Since the glycosidic-O was replaced with CH_2 in α-C-GalCer, α-C-GalCer could not be presented in human CD1d.

In summary, we have generated an NKT cell neoglycolipid ligand, α-carba-GalCer, the carbocyclic analogue of α-GalCer, by replacement of the 5a′-O of the pyranose ring of D-galactose with CH_2, by which the interaction between Pro28

at the CDR1 of TCRα chain and 5a'-CH_2 on galactose would be enhanced by the newly created hydrophobic interaction. Moreover, α-carba-GalCer possesses a stable ether linkage instead of a glycosyl (acetal) bond of α-GalCer, which would not be degraded by glycosidase, resulting in being more resistant against decomposition and maintained for a longer time than α-GalCer. These structural changes may increase their stable binding and result in potent induction of T_h1-biased cytokine production. Therefore, α-carba-GalCer would be a potential analogue to induce NKT cell-mediated adjuvant effects for protection against tumor malignancy or virus infection.

Funding

Grant-in-Aid for Young Scientists (B) (20790108) from the Ministry of Education, Culture, Sports, Science and Technology, Japan, to T.T.

Acknowledgements

The authors wish to thank Dr Peter Burrows for his critical reading and editing and Ms Norie Takeuchi for secretarial assistance.

References

1 Taniguchi, M., Harada, M., Kojo, S., Nakayama, T. and Wakao, H. 2003. The regulatory role of Valpha14 NKT cells in innate and acquired immune response. *Annu. Rev. Immunol.* 21:483.
2 Wilson, S. B. and Delovitch, T. L. 2003. Janus-like role of regulatory iNKT cells in autoimmune disease and tumour immunity. *Nat. Rev. Immunol.* 3:211.
3 Brigl, M., Bry, L., Kent, S. C., Gumperz, J. E. and Brenner, M. B. 2003. Mechanism of CD1d restricted natural killer T cell activation during microbial infection. *Nat. Immunol.* 4:1230.
4 Cui, J., Shin, T., Kawano, T. *et al.* 1997. Requirement for Vα14 NKT cells in IL-12-mediated rejection of tumors. *Science* 278:1623.
5 Fujii, S., Shimizu, K., Smith, C., Bonifaz, L. and Steinman, R. M. 2003. Activation of natural killer T cells by alpha-galactosylceramide rapidly induces the full maturation of dendritic cells *in vivo* and thereby acts as an adjuvant for combined CD4 and CD8 T cell immunity to a coadministered protein. *J. Exp. Med.* 198:267.
6 Dhodapkar, M. V. 2009. Harnessing human CD1d restricted T cells for tumor immunity: progress and challenges. *Front. Biosci.* 14:796.
7 Cerundolo, V. and Salio, M. 2007. Harnessing NKT cells for therapeutic applications. *Curr. Top. Microbiol. Immunol.* 314:325.
8 Wu, L. and Van Kaer, L. 2009. Natural killer T cells and autoimmune disease. *Curr. Mol. Med.* 9:4.
9 Koch, M., Stronge, V. S., Shepherd, D. *et al.* 2005. The crystal structure of human CD1d with and without alpha-galactosylceramide. *Nat. Immunol.* 6:819.
10 Zeng, Z., Castaño, A. R., Segelke, B. W., Stura, E. A., Peterson, P. A. and Wilson, I. A. 1997. Crystal structure of mouse CD1: an MHC-like fold with a large hydrophobic binding groove. *Science* 277:339.
11 Kawano, T., Cui, J., Koezuka, Y. *et al.* 1997. CD1d-restricted and TCR-mediated activation of Va14 NKT cells by glycosylceramides. *Science* 278:626.
12 McCarthy, C., Shepherd, D., Fleire, S. *et al.* 2007. The length of lipids bound to human CD1d molecules modulates the affinity of NKT cell TCR and the threshold of NKT cell activation. *J. Exp. Med.* 204:1131.
13 Oki, S., Chiba, A., Yamamura, T. and Miyake, S. 2004. The clinical implication and molecular mechanism of preferential IL-4 production by modified glycolipid-stimulated NKT cells. *J. Clin. Invest.* 113:1631.
14 Oki, S., Tomi, C., Yamamura, T. and Miyake, S. 2005. Preferential T(h)2 polarization by OCH is supported by incompetent NKT cell induction of CD40L and following production of inflammatory cytokines by bystander cells *in vivo*. *Int. Immunol.* 17:1619.
15 Tashiro, T., Nakagawa, R., Inoue, S. *et al.* 2007. RCAI-56, a carbocyclic analogue of KRN7000: its synthesis and potent activity for natural killer (NK) T cells to preferentially produce interferon-γ. *Tetrahedron Lett.* 48:3343.
16 Watarai, H., Nakagawa, R., Omori-Miyake, M., Dashtsoodol, N. and Taniguchi, M. 2008. Methods for detection, isolation and culture of mouse and human invariant NKT cells. *Nat. Protoc.* 3:70.
17 Yanagihara, S., Komura, E., Nagafune, J., Watarai, H. and Yamaguchi, Y. 1998. EBI1/CCR7 is a new member of dendritic cell chemokine receptor that is up-regulated upon maturation. *J. Immunol.* 161:3096.
18 Willcox, B. E., Gao, G. F., Wyer, J. R. *et al.* 1999. TCR binding to peptide-MHC stabilizes a flexible recognition interface. *Immunity* 10:357.
19 Zajonc, D. M., Cantu, C. 3rd, Mattner, J. *et al.* 2005. Structure and function of a potent agonist for the semi-invariant natural killer T cell receptor. *Nat. Immunol.* 6:810.
20 Schmieg, J., Yang, G., Franck, R. W. and Tsuji, M. 2003. Superior protection against malaria and melanoma metastases by a C-glycoside analogue of the natural killer T cell ligand a-galactosylceramide. *J. Exp. Med.* 198:1631.
21 Naidenko, O. V., Maher, J. K., Ernst, W. A., Sakai, T., Modlin, R. L. and Kronenberg, M. 1999. Binding and antigen presentation of ceramide-containing glycolipids by soluble mouse and human CD1d molecules. *J. Exp. Med.* 190:1069.
22 Liu, Y., Goff, R. D., Zhou, D. *et al.* 2006. A modified α-galactosyl ceramide for staining and stimulating natural killer T cells. *J. Immunol. Methods* 312:34.
23 Greten, T. F., Korangy, F., Neumann, G. *et al.* 2002. Peptide-beta2-microglobulin-MHC fusion molecules bind antigen-specific T cells and can be used for multivalent MHC-Ig complexes. *J. Immunol. Methods* 271:125.
24 Hayakawa, Y., Takeda, K., Yagita, H., Van Kaer, L., Saiki, I. and Okumura, K. 2001. Differential regulation of Th1 and Th2 functions of NKT cells by CD28 and CD40 costimulatory pathways. *J. Immunol.* 166:6012.
25 Sidobre, S., Naidenko, O. V., Sim, B. C., Gascoigne, N. R., Garcia, K. C. and Kronenberg, M. 2002. The V alpha 14 NKT cell TCR exhibits high-affinity binding to a glycolipid/CD1d complex. *J. Immunol.* 169:1340.
26 Houston, J. B. and Galetin, A. 2008. Methods for predicting *in vivo* pharmacokinetics using data from *in vitro* assays. *Curr. Drug Metab.* 9:940.
27 Li, X., Chen, G., Garcia-Navarro, R., Franck, R. W. and Tsuji, M. 2009. Identification of C-glycoside analogues that display a potent biological activity against murine and human invariant natural killer T cells. *Immunology* 127:216.
28 Lee, P. T., Benlagha, K., Teyton, L. and Bendelac, A. 2002. Distinct functional lineages of human V(alpha)24 natural killer T cells. *J. Exp. Med.* 195:637.
29 Borg, N. A., Wun, K. S., Kjer-Nielsen, L. *et al.* 2007. CD1d-lipid-antigen recognition by the semi-invariant NKT T-cell receptor. *Nature* 448:44.

Clinical & Experimental Immunology
The Journal of Translational Immunology
immunology

Inhibition of transforming growth factor-β signalling attenuates interleukin (IL)-18 plus IL-2-induced interstitial lung disease in mice

S. Segawa, D. Goto, Y. Yoshiga, M. Sugihara, T. Hayashi, Y. Chino, I. Matsumoto, S. Ito and T. Sumida
Division of Clinical Immunology, Doctoral Program in Clinical Sciences, Graduate School of Comprehensive Human Sciences, University of Tsukuba, Tsukuba, Ibaraki, Japan

Accepted for publication 15 December 2009
Correspondence: Takayuki Sumida, Division of Clinical Immunology, Doctoral Program in Clinical Sciences, Graduate School of Comprehensive Human Sciences, University of Tsukuba, 1-1-1, Tennoudai, Tsukuba, Ibaraki, 305-8575, Japan.
E-mail: tsumida@md.tsukuba.ac.jp

Summary

Interstitial lung disease (ILD) is an intractable disease induced by various factors in humans. However, there is no universally effective treatment for ILD. In this study, we investigated the role of transforming growth factor (TGF)-β signalling in the pathogenesis of ILD by using model mice. Injection of interleukin (IL)-18 plus IL-2 in C57BL6 (B6) mice resulted in acute ILD by infiltration of natural killer (NK) cells and a significant increase of TGF-β mRNA in the lung. To examine the pathogenetic role of TGF-β in ILD mice, we used SB-431542 (4-[4-(1,3-benzodioxol-5-yl)-5-(2-pyridinyl)-1H-imidazol-2-yl]-benzamide), which is a potent and selective inhibitor of TGF-β receptor I (TβRI), also known as activin receptor-like kinase 5 (ALK5). Treatment of B6-ILD mice with SB-431542 resulted in improvement of ILD, delay in mortality, reduction of the expression of interferon (IFN)-γ and IL-6 in the lungs. The same treatment also decreased significantly the percentage of natural killer (NK) cells in the lungs ($P < 0.05$) and mRNA expression levels of certain chemokines such as CCL2, CCL3, CCL4, CCL5 and CXCL10 in B6-ILD. These findings were confirmed by IL-18 plus IL-2 treatment of Smad3-deficient (Smad3$^{-/-}$) mice ($P < 0.05$). Our results showed that inhibition of TGF-β signalling reduced the percentage of NK cells and the expression of certain chemokines in the lungs, resulting in improvement of ILD. The findings suggest that TGF-β signalling may play an important role in the pathogenesis of IL-18 plus IL-2-induced ILD in mice.

Keywords: activin receptor-like kinase 5, chemokines, interstitial lung disease, pathogenesis, SB-431542, TGF-β signalling

Introduction

Interstitial lung disease (ILD) is an intractable disease induced by various factors such as autoimmune diseases, drugs, occupational and environmental exposure [1]. However, there is no universally effective treatment for ILD. On the other hand, chemotherapy with bleomycin (BLM) and busulphan is reported to cause lung fibrosis in some patients [2]. Histopathologically, diffuse infiltration of mononuclear and polymorphonuclear leucocytes is observed in the lung in the early stages of human ILD. Following the interstitial inflammation, florid fibroblast proliferation within both the interstitium and alveolar space is often detected. The same pathology is observed in BLM-induced ILD in mice [1]. Previous studies suggested that various mediators, such as cytokines and chemokines, including tumour necrosis factor (TNF)-α, transforming growth factor (TGF)-β, interleukin (IL)-1β, macrophage inflammatory factor (MIP)-1α/CCL3, monocyte chemoattractant protein (MCP)-1/CCL2, reactive oxygen species (ROS) and Fas/Fas ligand interactions, are associated with BLM-induced ILD and fibrosis in mice [3–9].

IL-18, a member of the IL-1 family, is a proinflammatory cytokine [10,11] known to induce interferon (IFN)-γ production synergistically by stimulation with IL-12, IL-2, antigens and IFN-α. Previous studies reported that IL-18 can potentially induce Th2 cytokines from T cells, natural killer (NK) cells, NK T cells, basophils and mast cells [11–16]. Thus, IL-18 can act as co-factor for both T helper type 1 (Th1) and Th2 cell development. In BLM-induced ILD mice models, there were two conflicting reports on the effect of IL-18. Nakatani-Okuda *et al.* [17] reported that IL-18 played a protective role in BLM-induced ILD in mice. In contrast, Hoshino *et al.* [18] reported that IL-18 played a

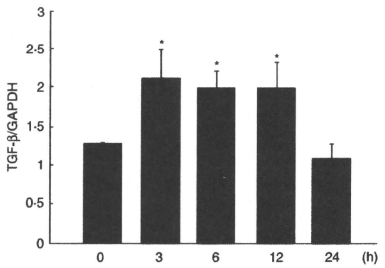

Fig. 1. Expression of transforming growth factor (TGF)-β mRNA after injection of interleukin (IL)-18 plus IL-2. Expression of TGF-β mRNA was analysed by real-time–polymerase chain reaction (RT-PCR). C57BL/6 (B6) mice were injected intraperitoneally with a single dose of IL-18/IL-2. At 3, 6, 12 and 24 h after injection, mice were killed and lung mRNA was extracted. Data are mean ± standard error of the mean; $n = 3$ mice per group. $^*P < 0{\cdot}05$; one-way analysis of variance.

pathologenetic role in the ILD. Therefore, the intimate role of IL-18 in ILD was controversial. Recently, Okamoto *et al.* [19] reported a new mouse model of ILD induced by IL-18 plus IL-2 (IL-18/IL-2). Daily administration of IL-18 with IL-2, but not IL-18 or IL-2 alone, produced a synergistic effect and induced ILD in mice. Unlike BLM-induced ILD, lung fibrosis was not caused in IL-18/IL-2-induced ILD. The pathological condition of BLM-induced ILD was mainly fibroblastic proliferation [20]. However, little fibroblastic proliferation was found in IL-18/IL-2-induced ILD. This model of ILD is characterized by severe infiltration of NK cells, mononuclear cells and polymorphonuclear leucocytes in the lung. Furthermore, the mortality in this two ILD mice models was different. Whereas 60% of mice died at 30 days after BLM treatment [21], 100% of mice died at 7 days after IL-18/IL-2 injection. Based on rapid and severe cell infiltration in IL-18/IL-2-induced ILD, the mouse model is considered suitable for early-phase human ILD.

Various chemokines, such as CCL2, CCL3, CCL4, CCL5, CXCL1 and CXCL8, are induced by activated fibroblasts in the lung tissue [22]. Mice with BLM-induced pulmonary fibrosis exhibit up-regulation of CCL2, CCL5, CCL3 and CXCL1 in the lung and such overexpression is associated with enhanced fibroblast proliferation and collagen production [23]. Thus, these chemokines are thought to be involved in the pathogenesis of ILD and subsequent fibrotic process. In contrast, the functional roles of chemokines in IL-18/IL-2-induced ILD in mice remain elusive, although lymphotactin (Ltn), CCL2, CCL3, CCL4, CCL5, CCL11, CXCL1 and CXCL10 are increased in the lung [19].

TGF-β is thought to be one of the pathogenic factors in ILD. Previous reports suggested that TGF-β acts as a regulatory molecule with pleiotropic effects on cell proliferation, differentiation, migration and survival [24]. TGF-β mediates its biological functions via binding to TGF-β receptor II (TβRII) and phosphorylation of TGF-β receptor I (TβRI), also known as activin receptor-like kinase 5 (ALK5). After forming the TGF-β–TβRII-ALK5 complex, ALK5 phosphorylates intracellular signal mediators Smad2/3. The importance of ALK5-mediated Smad2/3 activation in TGF-β signalling has been confirmed both *in vitro* and *in vivo* [24–29].

SB-431542 (4-[4-(1,3-benzodioxol-5-yl)-5-(2-pyridinyl)-1H-imidazol-2-yl]-benzamide) is a potent and selective inhibitor of ALK-5 [30–32]. Inhibition of ALK-5 suppressed BLM-induced pulmonary fibrosis [33]. However, the therapeutic potential of ALK-5 inhibitor in IL-18/IL-2-induced ILD has not yet been clarified.

In the present study, we examined the role of TGF-β signalling in early-stage ILD. For this purpose, we used SB-431542 and Smad3-deficient ($Smad3^{-/-}$) mice for IL-18/IL-2-induced ILD. The results demonstrated that inhibition of TGF-β signalling suppressed accumulation of NK cells and reduced mRNA expression of CCL2, CCL3, CCL4, CCL5 and CXCL10 in the lung. The main message of this study is that Smad-mediated TGF-β signalling seems to play an important role in the pathogenesis of IL-18/IL-2-induced ILD.

Materials and methods

Mice

C57BL/6 (B6) mice were purchased from Charles River Japan Inc. (Tokyo, Japan). Smad3-deficient ($Smad3^{-/-}$) mice were kindly provided by Dr Chuxia Deng (National Institute of Diabetes and Digestive and Kidney Diseases, Bethesda, MD, USA) [34]. The genotypes of both B6 and $Smad3^{-/-}$ mice were determined by polymerase chain reaction (PCR) analysis on tail DNA obtained from 4-week-old animals. Female mice were used in this study. The animals were kept under specific pathogen-free conditions and studied at 4–5 weeks of age. The Institutional Animal Care and Use Committee at Tsukuba University approved the experimental protocol.

Cell isolation and purification

Pulmonary lymphocytes were isolated as described previously [35], with the following modifications. The lung was perfused thoroughly with phosphate-buffered saline (PBS) to remove circulating blood cells. The dissected lung was minced in PBS containing 1 mM ethylenediamine tetraacetic acid (EDTA). The minced lung tissue was suspended in RPMI-1640 medium (Sigma-Aldrich, St Louis, MO, USA) containing 10% fetal bovine serum (FBS) (BioWest, FL, USA), 1 mM EDTA and 1 mM dithiothreitol (DTT). The suspension was incubated at 37°C for 45 min with gentle

shaking. The resultant suspension was passed through nylon mesh to remove debris. The washed and recovered cells were subjected to Lympholyte (Cedarlane, Ontario, Canada) at 1100 *g* at room temperature for 20 min. The resultant interface containing pulmonary lymphocytes was recovered and washed with RPMI-1640 medium containing 10% FBS, 100 units/ml penicillin, 100 μg/ml streptomycin and 50 μM 2-mercaptoethanol. Spleens were harvested and haemolyzed with PBS. Single-cell suspensions were prepared in RPMI-1640 medium containing 10% FBS, 100 units/ml of penicillin, 100 μg/ml streptomycin and 50 μM 2-mercaptoethanol.

Antibodies and flow cytometry

All antibodies were used according to the recommendations of the respective manufacturers. For flow cytometric analysis, cells were preincubated with anti-CD16/32 (eBioscience, San Diego, CA, USA) to block Fc receptors. The following antibodies were used in this study: phycoerythrin (PE)-conjugated anti-natural killer (NK)1·1 (PK136) (Biolegend, San Diego, CA, USA) and PE/cyanine 7 (Cy7)-conjugated anti-CD3ε (145-2C11) (Biolegend). The stained cells were analysed on CyAn advanced digital processing (ADP) (Dako, Glostrup, Denmark) and data were processed using Summit4·3 (Dako).

Induction of lung fibrosis with IL-18 and IL-2

Recombinant human IL-2 (rhIL-2) and recombinant mouse IL-18 (rmIL-18) were obtained from MBL (Nagoya, Japan). Mice were treated once a day with an intraperitoneal (i.p.) injection of rhIL-2 (100 000 U) and/or rmIL-18 (1 μg). These cytokines were suspended in sterile 200 μl PBS. Mice treated with 200 μl PBS served as the control group. Following treatment for 3 days, mice were bled and killed. Pulmonary lymphocytes and splenocytes were analysed by flow cytometry.

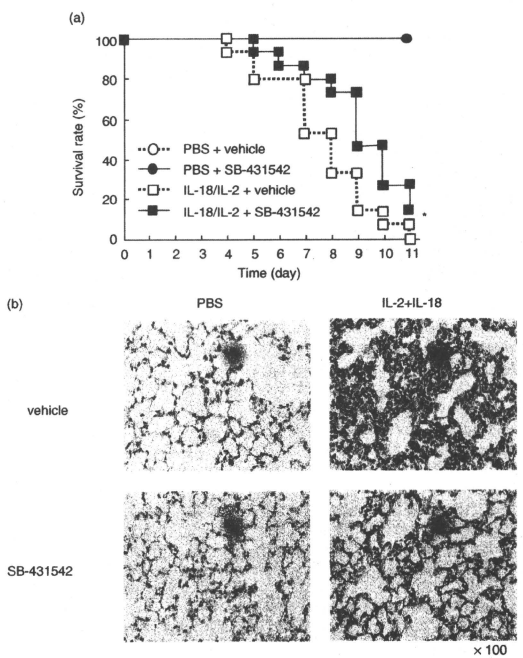

Fig. 2. Effects of SB-431542 in interleukin (IL)-18 plus IL-2-induced interstitial lung disease (ILD) mice. (a) B6 mice were injected with IL-18/IL-2 with or without SB-431542 for 10 days, as described in Materials and methods. ○, phosphate = interstitial lung disease (ILD) –buffered saline (PBS) + vehicle; ●, PBS + SB-431542; □, IL-18/IL-2 + vehicle; ■, IL-18/IL-2 + SB-431542; $n = 5$ mice per group. Data are representative of three independent experiments and graph shows pooled data of three experiments. $^*P < 0{\cdot}05$; Kaplan–Meier method. (b) Lungs were harvested from B6 mice at 24 h after injected with IL-18/IL-2 with or without SB-431542 for 3 days. Lung tissues were stained with haematoxylin and eosin. Original magnification: ×100. (c) Lungs were harvested from B6 mice at 6 h after injection with IL-18/IL-2 with or without SB-431542 for 3 days. (d) The sera were harvested from B6 mice at 6 h after injection with IL-18/IL-2 with or without SB-431542 for 3 days. Serum cytokine levels were measured by enzyme-linked immunosorbent assay (ELISA). ELISA assayed the lung tissue supernatant as described in Materials and methods. Date are mean ± standard error of the mean; $n = 3$ mice per group. $^*P < 0{\cdot}05$; Student's *t*-test.

Treatment of mice with SB-431542

ALK-5 inhibitor, SB-431542 (4-[4-(1,3-benzodioxol-5-yl)-5-(2-pyridinyl)-1H-imidazol-2-yl]-benzamide) (SB-431542) was obtained from Tocris Bioscience (Park Ellisville, MO, USA). It was suspended in sterile dimethyl sulphoxide (DMSO) at 20 mg/ml. Mice were treated twice a day (0 h and 12 h after IL-18/IL-2 treated) by i.p. injection of 50 µl (0·2 mg) SB-431542 or vehicle for 3 days.

Reverse transcription polymerase chain reaction (RT-PCR) analysis

Total RNA was extracted from the lung, and was reverse transcribed into cDNA using RevertAid™ first-strand cDNA synthesis kit (Fermentas, Burlington, Ontario, Canada), according to the manufacturer's protocol. For amplification of chemokine cDNA, after an initial denaturation step at 94°C for 4 min, 35 cycles were conducted each at 94°C for 30 s followed by 60°C for 30 s and 72°C for 30 s, and further extension at 72°C for 7 min. For amplification of glyceraldehyde-2-phosphate dehydrogenase (GAPDH) cDNA, PCR assays were performed for 30 cycles (94°C for 30 s followed by 60°C for 30 s and 72°C for 30 s). At the end of cycles, samples were stored at 4°C until analysed. After amplification, the PCR products were separated by electrophoresis in 2·0% agarose gels. The primer sequences were as follows and the PCR product sizes [base pairs (bp)] were indicated: CCL2, 5′-AGGTCCCTGTCATGCTTCTG, 3′-TCTGGACCCATTCCTTCTTG (249 bp); CCL3, 5′-AGATTCCACGCCAATTCATC, 3′-CTCAAGCCCCTGCTCTACAC (223 bp); CCL4, 5′-CCCACTTCCTGCTGTTTCTC, 3′-GAGGAGGCCTCTCCCTGAAGT (238 bp); CCL5, 5′-CCCTCACCATCATCCTCACT, 3′-CCTTCGAGTGACAAACACGA (185 bp); CCL11, 5′-TCCACAGCGCTTCTATTCCT, 3′-CTATGGCTTTCAGGGTGCAT (178 bp); CXCL1, 5′-GCTGGGATTCACCTCAAGAA, 3′-TCTCCGTTACTTGGGGACAC (180 bp); CXCL10, 5′-GGATGGCTGTCCTAGCTCTG, 3′-ATAACCCCTTGGGAAGATGG (211 bp); and GAPDH, 5′-CGTCCCGTAGACAAAATGGGT, 3′-GAATTTGCCGTGAGTGGAGT (177 bp).

Quantification of gene expression by RT-PCR

The cDNA samples were amplified with specific primers and fluorescence-labelled probes for the target genes. Specific primers and probes for TGF-β and GAPDH were purchased from Applied Biosystems Japan (Tokyo, Japan). The amplified product genes were monitored on an ABI 7700 sequence detector (Applied Biosystems Japan). The quantitative PCR master mix was purchased from Applied Biosystems Japan. The final concentrations of the primers were 200 nM for each of the 5′ and 3′ primers, and the final probe concentration was 100 nM. The thermal cycler conditions used were 50°C for 2 min, 95°C for 10 min, then 50 cycles of 95°C for 15 s and 60°C for 1 min. Serial dilutions of a standard sample were included in every assay, and standard curves for the genes of interest and GAPDH genes were generated. All measurements were performed in triplicate. The level of gene expression was calculated from the

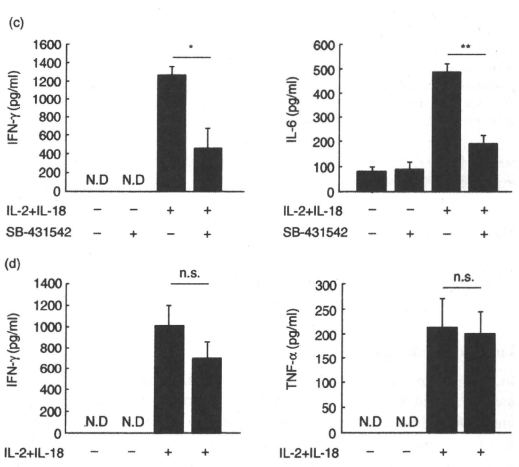

Fig. 2. *Continued*

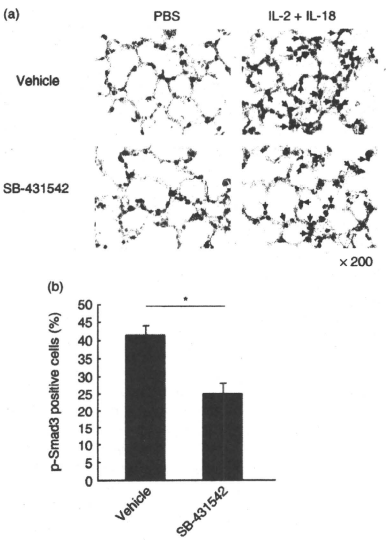

Fig. 3. Immunohistochemical findings of phosphorylated Smad3 (p-Smad3) in lungs of B6 mice treated with SB-431542. (a) Lungs were harvested from B6 mice at 6 h after treatment with interleukin (IL)-18/IL-2 with or without SB-431542 for 3 days. The tissues were stained immunohistochemically with anti-pSmad3 antibody. Arrow: pSmad3-positive cells. Original magnification: ×200. (b) In lungs of mice treated with IL-18/IL-2 with or without SB-431542, the percentage of p-Smad3-positive cells per total cells was calculated in five fields under ×200 magnification. Data are mean ± standard error of the mean of three mice per group. $^*P < 0{\cdot}05$; Student's *t*-test.

standard curve, and expressed relative to GAPDH gene expression.

Histological examination

For histological analysis, mice were euthanized by isopropanol and lung was fixed with 4% paraformaldehyde. Lung tissues were stained with haematoxylin and eosin (H&E).

Immunohistochemistry

In the present study, anti-phosphorylated Smad3 were used (Rockland, Gilbertsville, PA, USA). For detection of immunocomplexes, Histofine (Nichirei Corporation, Tokyo, Japan) for phosphorylated Smad3 was used using the manufacturer's instructions. Substitution of the primary antibody with irrelevant immunoglobulin G (IgG) served as negative controls. Staining was repeated for each sample at least three times. After counterstaining with haematoxylin, sections were mounted with mounting agent, PARAmount-D (Falma, Tokyo, Japan).

Measurement of cytokines in the lung and serum

For enzyme-linked immunosorbent assay (ELISA), the lung tissue was suspended and homogenized in sterile PBS and centrifuged at 10 000 *g* for 10 min. The cytokine levels in the lung tissue supernatants and the serum were evaluated by ELISA (R&D Systems, Minneapolis, MN, USA).

Statistical analysis

Data are expressed as median or mean ± standard error of the mean (s.e.m.). Data were analysed using a statistical software package (StatView 5·0; SAS Institute Inc, Cary, NC, USA). The survival rates were analysed by Kaplan–Meier method. Differences between groups were examined for statistical significance using Student's *t*-test. For multiple group comparisons, one-way analysis of variance (ANOVA) was performed followed by a *post-hoc* Dunnett's test. A *P*-value less than 0·05 denoted a statistically significant difference.

Results

Overexpression of TGF-β mRNA in IL-18/IL-2-induced ILD

Figure 1 shows significant up-regulation of TGF-β mRNA in the whole lung tissues from mice at 3, 6 and 12 h after injection of IL-18/IL-2 compared with 0 h ($P < 0{\cdot}05$, $P < 0{\cdot}01$ and $P < 0{\cdot}05$, respectively). However, at 24 h after injection of IL-18/IL-2, the expression of TGF-β mRNA returned to the level at 0 h.

SB-431542 ameliorated ILD and reduced the expression of IFN-γ and IL-6 in the lung

Treatment with SB-431542 was employed to examine the effect of TGF-β inhibition on IL-18/IL-2-induced ILD. As shown in Fig. 2a, treatment with SB-431542 delayed mortality significantly compared with control on the 11th day ($P < 0{\cdot}05$). Histological examination showed inhibition of cell infiltration in the lungs of SB-431542-treated ILD mice compared with the control (Fig. 2b). Furthermore, we analysed the expression of cytokines in sera and the lung tissues from SB-431542 and vehicle-treated ILD-induced mice. In the lung of SB-431542-treated mice, the expression of IFN-γ and IL-6 was significantly lower than control mice ($P < 0{\cdot}05$, $P < 0{\cdot}01$, Fig. 2c). However, in sera, the expression of IFN-γ and TNF-α was not different in each group (Fig. 2d). The lung wet–dry ratio was not significantly different between SB-431542-treated ILD mice and vehicle-treated ILD mice (data not shown).

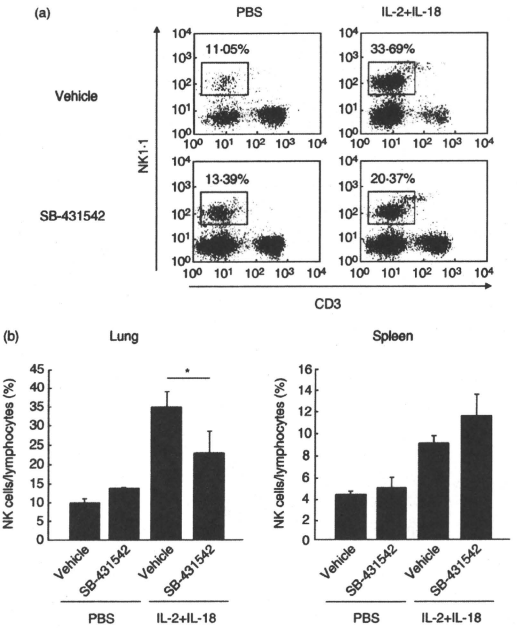

Fig. 4. Flow cytometric analysis of pulmonary lymphocytes in B6 mice treated with SB-431542. (a) Pulmonary lymphocytes were harvested from B6 mice at 24 h after treatment with interleukin (IL)-18/IL-2 with or without SB-431542 for 3 days, as described in Materials and methods. Pulmonary lymphocytes were stained with phycoerythrin (PE)-conjugated anti-natural killer (NK)1·1 and PE/cyanine 7 (Cy7)-conjugated anti-CD3ε monoclonal antibodies. (b) Left: proportion of NK cells relative to pulmonary lymphocytes in mice treated with IL-18/IL-2 and with or without SB-431542. Right: proportion of NK cells relative to splenocytes in B6 mice treated with IL-18/IL-2 with or without SB-431542. Data are mean ± standard error of the mean of three mice per group. *$P < 0·05$; Student's *t*-test.

SB-431542 ameliorates lowers percentage of phosphorylated Smad3-positive cells

Furthermore, the number of phosphorylated Smad3-positive cells was lower in the lung of B6 mice treated with SB-431542 compared with the control (Fig. 3a). To confirm this result, we counted the percentage of p-Smad3-positive cells relative to the total number of cells. The percentage of p-Smad3-positive cells was significantly lower in SB-431542-treated ILD mice (24·98 ± 6·11%) compared with the control (41·12 ± 4·92%, $P < 0·05$, Fig. 3b).

SB-431542 significantly reduces NK cells in the lung

The results showed significantly fewer NK cells (22·53 ± 5·90%) in the lungs of SB-431542-treated B6 mice compared with the control (34·84 ± 4·43%, $P < 0·05$, Fig. 4a and b). In contrast, the percentage of NK cells in splenocytes of SB-431542-treated B6 mice (11·50 ± 2·13%) tended to be higher than the control (8·99 ± 0·82%, Fig. 4b).

Improvement of ILD and reduced cell infiltration in lungs of Smad3$^{-/-}$ mice

We also conducted experiment in Smad3$^{-/-}$ mice for further assessment of the role of TGF-β signalling on IL-18/IL-2-induced ILD [31]. Histological examination showed milder cell infiltration in the lungs of Smad3$^{-/-}$ mice compared with the control (Fig. 5a). Furthermore, flow cytometry showed a significantly small proportion of NK cells in the lung of Smad3$^{-/-}$ mice treated with IL-18/IL-2 (22·77 ± 3·27%) compared with B6 mice (33·89 ± 5·06%, $P < 0·05$, Fig. 5b and c).

Underexpression of chemokine mRNAs in lung of SB-431542-treated and Smad3$^{-/-}$ mice

RT-PCR showed that the expression levels of CCL2, CCL3, CCL4, CCL5 and CXCL10 mRNAs were lower in the lungs of B6 mice treated with SB-431542 than the control (Fig. 6a). Furthermore, the expression levels of CCL2, CCL3, CCL4, CCL5, CCL11, CXCL1 and CXCL10 were lower in the lungs of Smad3$^{-/-}$ mice than the control (Fig. 6b).

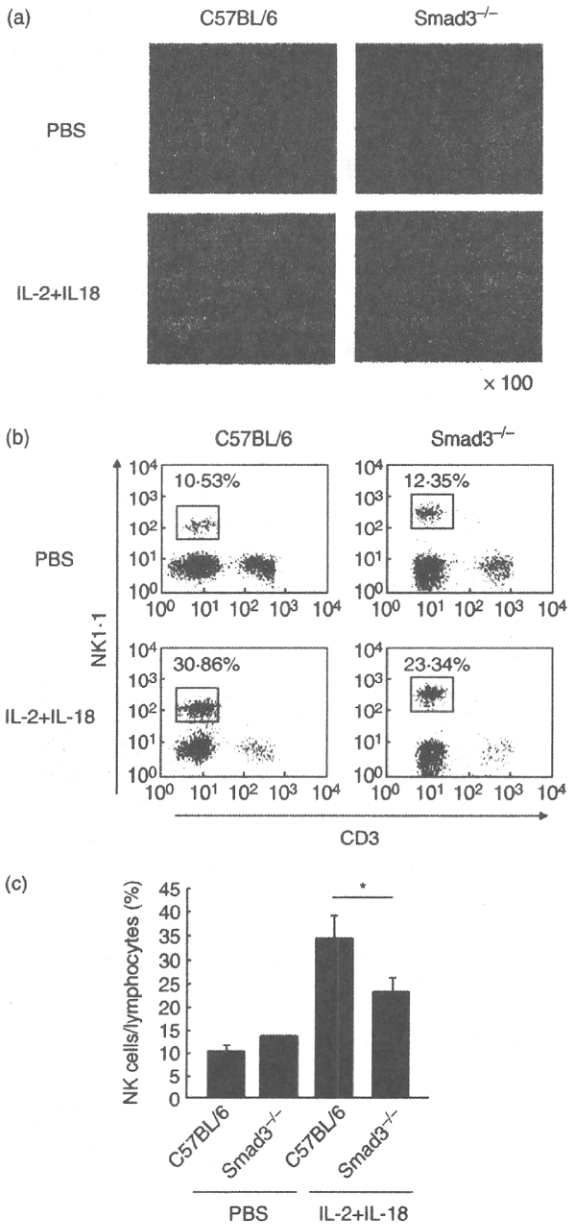

Fig. 5. Histological and flow cytometric analysis of pulmonary lymphocytes in Smad3$^{-/-}$ mice. (a) Lungs were harvested from B6 and Smad3$^{-/-}$ mice at 24 h after treated with interleukin (IL)-18/IL-2 for 3 days. Lung tissues were stained with haematoxylin and eosin. Original magnification: ×100. (b) Pulmonary lymphocytes were harvested from B6 and Smad3$^{-/-}$ mice at 24 h after treatment with IL-18/IL-2 for 3 days, as described in Materials and methods. Pulmonary lymphocytes were stained with phycoerythin (PE)-conjugated anti-natural killer (NK)1·1 and PE/cyanine 7 (Cy7)-conjugated anti-CD3ε monoclonal antibodies. (c) Proportion of NK cells relative to pulmonary lymphocytes in B6 and Smad3$^{-/-}$ mice treated with IL-18/IL-2. Data are mean ± standard error of the mean of three mice per group. *$P < 0.05$; Student's *t*-test.

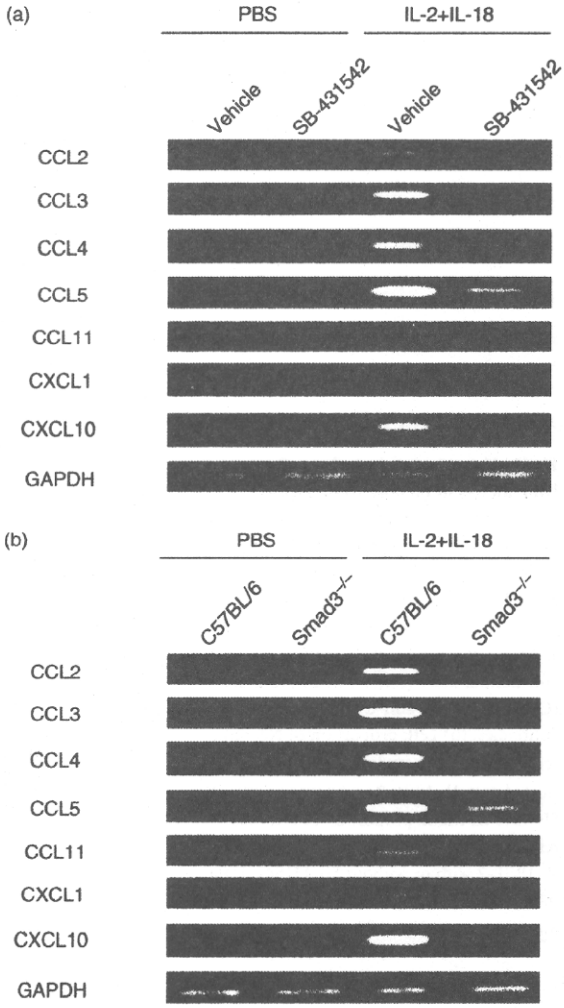

Fig. 6. Expression of chemokine mRNAs in lungs of mice deficient in transforming growth factor (TGF)-β. (a) mRNA expression of various chemokines in the lungs of B6 mice treated with SB-431542 and control mice. Lungs were removed at 24 h after the final dose of SB-431542 or vehicle and total RNA was extracted. Chemokine expression (CCL2, CCL3, CCL4, CCL5, CCL11, CXCL1 and CXCL10) was detected by reverse transcription polymerase chain reaction (RT-PCR). (b) mRNA expression of various chemokines in the lungs of Smad3$^{-/-}$ mice and control mice. Lungs were removed at 24 h after the third injection of interleukin (IL)-18/IL-2 and total RNA was extracted. Chemokine expression (CCL2, CCL3, CCL4, CCL5, CCL11, CXCL1 and CXCL10) was detected by RT-PCR. Representative results are shown of three experiments with similar findings.

Discussion

IL-18 and IL-2 are important cytokines that can induce IFN-γ production by NK cells [11]. IL-18 and IL-2 administered daily acted synergistically to induce ILD. ILD mice show severe infiltration of NK cells in the lungs and have high levels of IFN-γ in both serum and lung [19]. Depletion of NK cells by anti-NK1·1 monoclonal antibody or anti-asialo GM1 antibody treatment prevented this effect. Furthermore, the morbid effects of IL-18 and IL-2 were reduced in IFN-γ-deficient mice. These findings suggest that the increase of NK cells and elevation of IFN-γ seem to play a role in the pathogenesis of IL-18/IL-2-induced ILD in mice.

In other mouse models of ILD, BLM induces pulmonary fibrosis and the TGF-β pathway plays an important role in the pathogenesis of ILD [24,27–29,36]. The present study also showed increased expression of TGF-β mRNA in the lung in the early stage of ILD after injection of IL-18/IL-2. Thus, TGF-β seems to be involved in the pathogenesis of IL-18/IL-2-induced ILD and BLM-induced pulmonary fibrosis. Surprisingly, mice treated with SB-431542 delayed mortality in IL-18/IL-2-induced ILD. In addition, IL-18/IL-2-induced NK cell infiltration in the lung was decreased significantly following treatment with SB-431542 and also in Smad3$^{-/-}$ mice. Histological analysis demonstrated that SB-431542 reduced cell infiltration significantly in ILD mice. It was reported that injection of IL-18/IL-2 induced the expression of IFN-γ and TNF-α in sera, and IFN-γ and IL-6 in the lung [19]. In the lung, treatment with SB-431542 reduced the expression of IFN-γ and IL-6 from IL-18/IL-2-induced ILD mice, but in sera the expression of IFN-γ and TNF-α was not changed. Furthermore, IL-18/IL-2-induced ILD was improved in Smad3$^{-/-}$ mice. These findings indicate the involvement of Smad-mediated TGF-β signalling in the pathogenesis of murine ILD.

Bellone *et al.* [37] reported that TGF-β inhibited activated NK cells *in vitro*. Our preliminary study confirmed that exogenously added TGF-β suppressed NK cells *in vitro* (data not shown). However, in the present study, we demonstrated that shutdown of TGF-β signalling by SB-431542 or Smad3 knock-out down-regulated NK cells migration into the lung *in vivo*, indicating that TGF-β enhanced the infiltration of NK cells into the lung. The discrepancy might be due to the difference between the effects of TGF-β on NK cells *in vitro* and those *in vivo*. We proposed that TGF-β could enhance the migration of NK cells into the lung *in vivo*, whereas TGF-β suppressed the proliferation of NK cells *in vitro*.

Okamoto *et al.* [19] showed that certain chemokines, such as CCL2, CCL3, CCL4, CCL5, CCL11, CXCL1 and CXCL10, were up-regulated in the lungs of IL-18/IL-2-induced ILD mice. In contrast, in the lungs of B6 mice treated with SB-431542 and in Smad3$^{-/-}$ mice, chemokine mRNAs were down-regulated. Interestingly, larger proportions of NK cells were noted in the spleens of SB-431542-treated mice with ILD, although their proportion in the lungs was reduced. The latter finding may be due to redistribution and accumulation of NK cells in the spleen. Thus, inhibition of TGF-β signalling could, potentially, be a useful therapeutic strategy in ILD through regulation of NK cells infiltration in the lung.

In conclusion, the present study showed that inhibition of TGF-β signalling regulated IL-18/IL-2-induced ILD through inhibition of NK cells and down-regulation of certain chemokines in the lung. These findings support the notion that TGF-β signalling plays an important role in the pathogenesis of ILD.

Acknowledgements

We thank Dr Chuxla Deng (National Institute of Diabetes and Digestive and Kidney Diseases, MD) for kindly providing Smad3 deficient (Smad3$^{-/-}$) mice, and Dr F. G. Issa, for the critical reading of the manuscript. This study was supported in part by a Grant-in-Aid for Scientific Research by Japan Society for the Promotion of Science and the Japanese Ministry of Health, Labour and Welfare.

Disclosure

None of the authors has any conflict of interest with the subject matter or materials discussed in the manuscript.

References

1 King TE Jr. Clinical advances in the diagnosis and therapy of the interstitial lung diseases. Am J Respir Crit Care Med 2005; **172**:268–79.
2 Luna MA, Bedrossian CW, Lichtiger B, Salem PA. Interstitial pneumonitis associated with bleomycin therapy. Am J Clin Pathol 1972; **58**:501–10.
3 Piguet PF, Collart MA, Grau GE, Kapanci Y, Vassalli P. Tumor necrosis factor/cachectin plays a key role in bleomycin-induced pneumopathy and fibrosis. J Exp Med 1989; **170**:655–63.
4 Nakao A, Fujii M, Matsumura R *et al.* Transient gene transfer and expression of smad7 prevents bleomycin-induced lung fibrosis in mice. J Clin Invest 1999; **104**:5–11.
5 Scheule RK, Perkins RC, Hamilton R, Holian A. Bleomycin stimulation of cytokine secretion by the human alveolar macrophage. Am J Physiol 1992; **262**:386–91.
6 Smith RE, Strieter RE, Phan SH *et al.* Production and function of murine macrophage inflammatory protein-1 alpha in bleomycin-induced lung injury. J Immunol 1994; **153**:4704–12.
7 Zhang K, Gharaee-Kermani M, Jones ML, Warren JS, Phan SH. Lung monocyte chemoattractant protein-1 gene expression in bleomycin-induced pulmonary fibrosis. J Immunol 1994; **153**:4733–41.
8 Hoshino T, Nakamura H, Okamoto M *et al.* Redox-active protein thioredoxin prevents proinflammatory cytokine- or bleomycin-induced lung injury. Am J Respir Crit Care Med 2003; **168**:1075–83.
9 Kuwano K, Hagimoto N, Kawasaki M *et al.* Essential roles of the Fas-Fas ligand pathway in the development of pulmonary fibrosis. J Clin Invest 1999; **104**:13–19.

10 Nakamishi K, Yoshimoto T, Tsustumi H, Okamura H. Interleukin-18 regulates both th1 and th2 response. Annu Rev Immunol 2001; **19**:423–74.

11 Hoshino T, Robert H, Wiltrout RH, Young HA. IL-18 is a potent coinducer of IL-13 in NK and T cells: a new potential role for IL-18 in modulating the immune response. J Immunol 1999; **162**:5070–7.

12 Hoshino T, Yagita H, Ortaldo JR, Wiltrout RH, Young HA. *In vivo* administration of IL-18 can induce IgE production through TH2 cytokine induction and up-regulation of CD40 ligand (CD154) expression on CD4+ T cells. Eur J Immunol 2000; **30**:1998–2006.

13 Hoshino T, Kawase Y, Okamoto M *et al.* IL-18- transgenic mice: *in vivo* evidence of a broad role for IL-18 in modulating immune function. J Immunol 2001; **166**:7014–18.

14 Wild JS, Sigounas A, Sur N *et al.* IFN-gamma-inducing factor (IL-18) increases allergic sensitization, serum IgE, Th2 cytokines, and airway eosinophilia in a mouse model of allergic asthma. J Immunol 2000; **164**:2701–10.

15 Yoshimoto T, Min B, Sugimoto T *et al.* Nonredundant roles for CD1d-restricted natural killer T cells and conventional CD4+ T cells in the induction of immunoglobulin E antibodies in response to interleukin 18 treatment of mice. J Exp Med 2003; **197**:997–1005.

16 Sims JE. IL-1 and IL-18 receptors, and their extended family. Curr Opin Immunol 2002; **14**:117–22.

17 Nakatani-Okuda A, Ueda H, Kashiwamura S *et al.* Protection against bleomycin-induced lung injury by IL-18 in mice. Am J Physiol Lung Cell Mol Physiol 2005; **289**:280–7.

18 Hoshino T, Okamoto M, Sakazaki Y, Kato S, Young HA, Aizawa H. Role of proinflammatory cytokines IL-18 and IL-1β in bleomycin-induced lung injury in humans and mice. Am J Respir Cell Mol Biol 2009; **41**:661–70.

19 Okamoto M, Kato S, Oizumi K *et al.* Interleukin18 (IL-18) in synergy with IL-2 induced lethal lung injury in mice: a potential role for cytokines, chemokines, and natural killer cells in the pathogenesis of interstitial pneumonia. Blood 2002; **99**:1289–98.

20 Chen ES, Greenlee BM, Wills-Karp M, Moller DR. Attenuation of lung inflammation and fibrosis in interferon-gamma-deficient mice after intratracheal bleomycin. Am J Respir Cell Mol Biol 2001; **24**:545–55.

21 Yang HZ, Cui B, Liu HZ *et al.* Targeting TLR2 attenuates pulmonary inflammation and fibrosis by reversion of suppressive immune microenvironment. J Immunol 2009; **182**:692–702.

22 Suzuki T, Chow CW, Downey GP. Role of innate cells and their products in lung immunopathology. Int J Biochem Cell Biol 2008; **40**:1348–61.

23 Kakizaki T, Kohno M, Watanabe M *et al.* Exacerbation of bleomycin-induced injury and fibrosis by pneumonectomy in the residual lung of mice. J Surg Res 2009; **154**:336–44.

24 Li MO, Wan YY, Sanjabi S, Robertson AK, Flavell RA. Transforming growth factor-β regulation of immune responses. Ann Rev Immunol 2006; **24**:99–146.

25 Bonniaud P, Kolb M, Galt T *et al.* Smad3 null mice develop airspace enlargement and are resistant to TGF-β-mediated pulmonary fibrosis. J Immunol 2004; **173**:2099–108.

26 Higashiyama H, Yoshimoto D, Okamoto Y, Kikkawa H, Asano S, Kinoshita S. Receptor-activated Smad localization in bleomycin-induced pulmonary fibrosis. J Clin Pathol 2007; **60**:283–9.

27 Venlatesan N, Pini L, Ludwig MS. Changes in Smad expression and subcellular localization in bleomycin-induced pulmonary fibrosis. Am J Physiol Lung Cell Mol Physiol 2004; **287**:L1342–7.

28 Zhao Y, Geverd DA. Regulation of Smad3 expression in bleomycin-induced pulmonary fibrosis: a negative feedback loop of TGF-β signaling. Biochem Biophys Res Commun 2002; **294**:319–23.

29 Zhao J, Shi W, Wang YL *et al.* Smad3 deficiency attenuates bleomycin-induced pulmonary fibrosis in mice. Am J Physiol Lung Cell Mol Physiol 2002; **282**:L585–93.

30 Laping NJ, Grygielko E, Mathur A *et al.* Inhibition of transforming growth factor (TGF)-β1-induced extracellular matrix with a novel inhibitor of the TGF-β type I receptor kinase activity: SB-431542. Mol Pharmacol 2002; **62**:58–64.

31 Inman GJ, Nicolás FJ, Callahan JF *et al.* SB-431542 is a potent and specific inhibitor of transforming growth factor-β superfamily type I activin receptor-like kinase (ALK) receptors ALK4, ALK5, and ALK7. Mol Pharmacol 2002; **62**:65–74.

32 Matsuyama S, Iwadate M, Kondo M *et al.* SB-431542 and Gleevec inhibit transforming growth factor-β-induced proliferation of human osteosarcoma cells. Cancer Res 2003; **63**:7791–8.

33 Higashiyama H, Yoshimoto D, Kaise T *et al.* Inhibition of activin receptor-like kinase 5 attenuates bleomycin-induced pulmonary fibrosis. Exp Mol Pathol 2007; **83**:39–46.

34 Yang X, Letterio JJ, Lechleider RJ *et al.* Targeted disruption of SMAD3 results in impaired mucosal immunity and diminished T cell responsiveness to TGF-beta. EMBO J 1999; **18**:1280–91.

35 Li S, Kishihara K, Akashi N *et al.* Vδ1$^+$ T cells are crucial for repertoire formation of γδ T cells in the lung. Biochem Biophys Res Commun 2008; **365**:246–51.

36 Batram U, Speer CP. The role of transforming growth factor beta in lung development and disease. Chest 2004; **125**:754–65.

37 Bellone G, Aste-Amezage M, Trinchieri G, Rodeck U. Regulation of NK cell functions by TGF-β1. J Immunol 1995; **155**:1066–73.

British Journal of Pharmacology (2010), 160, 292–310

0007-1188/10
www.brjpharmacol.org

RESEARCH PAPER

A novel antagonist of the prostaglandin E_2 EP_4 receptor inhibits Th1 differentiation and Th17 expansion and is orally active in arthritis models

Q Chen[1]*, K Muramoto[2]*, N Masaaki[2], Y Ding[1], H Yang[1], M Mackey[1], W Li[1], Y Inoue[2], K Ackermann[1], H Shirota[1], I Matsumoto[3], M Spyvee[1], S Schiller[1], T Sumida[3], F Gusovsky[1] and M Lamphier[1]

[1]*Eisai Research Institute of Boston, Andover, MA, USA,* [2]*Tsukuba Research Laboratories, Ibaraki, Japan, and* [3]*Department of Clinical Immunology, Graduate School of Comprehensive Human Science, University of Tsukuba, Tsukuba, Japan*

Background and purpose: Rheumatoid arthritis (RA) is an autoimmune disorder involving subsets of activated T cells, in particular T helper (Th) 1 and Th17 cells, which infiltrate and damage tissues and induce inflammation. Prostaglandin E_2 (PGE_2) enhances the Th17 response, exacerbates collagen-induced arthritis (CIA) and promotes inflammatory pain. The current study investigated whether selective antagonism of the PGE_2 EP_4 receptor would suppress Th1/Th17 cell development and inflammatory arthritis in animal models of RA.

Experimental approach: Effects of PGE_2 and a novel EP_4 receptor antagonist ER-819762 on Th1 differentiation, interleukin-23 (IL-23) production by dendritic cells (DCs), and Th17 development were assessed *in vitro*. The effect of ER-819762 was evaluated in CIA and glucose-6-phosphate isomerase (GPI)-induced arthritis models. In addition, the effects of ER-819762 on pain were evaluated in a model of chronic inflammatory pain induced by complete Freund's adjuvant (CFA) in the rat.

Key results: Stimulation of the EP_4 receptor enhanced Th1 differentiation via phosphatidylinositol 3 kinase signalling, selectively promoted Th17 cell expansion, and induced IL-23 secretion by activated DCs, effects suppressed by ER-819762 or anti-PGE_2 antibody. Oral administration of ER-19762 suppressed Th1 and Th17 cytokine production, suppressed disease in collagen- and GPI-induced arthritis in mice, and suppressed CFA-induced inflammatory pain in rats.

Conclusion and Implications: PGE_2 stimulates EP_4 receptors to promote Th1 differentiation and Th17 expansion and is critically involved in development of arthritis in two animal models. Selective suppression of EP_4 receptor signalling may have therapeutic value in RA both by modifying inflammatory arthritis and by relieving pain.

British Journal of Pharmacology (2010) **160**, 292–310; doi:10.1111/j.1476-5381.2010.00647.x

Keywords: PGE_2; EP_4 receptor; EP_4 antagonist; Th1; Th17; IFN-γ; IL-17; IL-23; CIA; GPI-induced arthritis model

Abbreviations: BSA, bovine serum albumin; CIA, collagen-induced arthritis; CFA, complete Freund's adjuvant; CRE, cAMP response elements; ER-819762, (*S*)-1′-(3,5-dimethylbenzyl)-2-ethyl-7,9-dimethoxy-10-methyl-5,10-dihydrospiro[benzo[e]imidazo[1,5-a]azepine-1,4′-piperidin]-3(2H)-one; FBS, fetal bovine serum; GPCR, G protein-coupled receptors; GPI, glucose-6-phosphate isomerase; IBMX, isobutylmethylxanthine; imDC, immature human dendritic cell; PGE_2, prostaglandin E_2; PI3K, phosphatidylinositol 3-kinase; PLAP, placental-like alkaline phosphatase; RA, rheumatoid arthritis; Th1, T helper 1; Th17, T helper 17; TLR, Toll-like receptor

Introduction

Rheumatoid arthritis (RA) is a chronic autoimmune disorder that is estimated to affect up to 1% of the population worldwide (Williams, 2006). Although not life-threatening, RA is a painful and debilitating disease that progressively limits the ability of patients to carry on normal lives. The factors that trigger this disease are not well understood but are believed to include both genetic and environmental components. Over the last decade, novel discoveries into the regulation of the immune system have permitted a better understanding of the development of autoimmunity. Upon encountering antigen, T helper (Th) cells differentiate into several subtypes, depending on various factors such as the cytokines produced, the consequent activation of intracellular signalling pathways,

Correspondence: Qian Chen, Eisai Research Institute of Boston Inc., 4 Corporate Drive, Andover, MA 01810 USA. E-mail: qian_chen@eisai.com
*These authors contributed equally to this work.
Received 30 June 2009; revised 2 November 2009; accepted 9 November 2009

and the expression of transcription factors. Among these T cell subtypes, Th1 and Th17 cells have been shown to be critically involved in the development of autoimmunity (Schulze-Koops and Kalden, 2001; Fouser *et al.*, 2008). While the molecular mechanisms controlling the differentiation and expansion of these T cell subsets have begun to be elucidated, specific agents to suppress the function of these critical T cell subtypes are only in early-stage development.

Prostaglandin E_2 (PGE_2) is an arachidonic acid metabolite that acts as a potent biological mediator, exerting its effects via activation of membrane G protein-coupled receptors (GPCRs). There are four receptor subtypes ($EP_{1,\ 2,\ 3}$ and $_4$; nomenclature follows Alexander *et al.*, 2009) which selectively bind PGE_2 and mediate its effects: Activation of EP_1 receptors leads to the influx of calcium. Activation of EP_3 receptors can induce a variety of signalling events depending on the particular EP_3 splicing variant being expressed, with inhibition of adenylate cyclase activity via Gi being the most common effect. EP_2 and EP_4 receptors induce Gs-mediated activation of adenylate cyclase and a subsequent increase in intracellular cyclic AMP (cAMP). In addition, EP_4 receptors activate the phosphatidylinositol 3-kinase (PI3K) signalling pathway (Fujino *et al.*, 2003). PGE_2 is known to play important roles in mediating many inflammatory responses and is often found at increased concentrations under a variety of inflammatory conditions (Hata and Breyer, 2004). Many reports suggest that PGE_2, via the induction of intracellular cAMP, can suppress pro-inflammatory T cell function, including T cell receptor signalling and consequent production of interleukin (IL)-2 (Mustelin and Tasken, 2003; Chemnitz *et al.*, 2006). PGE_2 has also been implicated in T-cell differentiation and is reported to inhibit Th1 but not Th2 cytokines via the induction of intracellular cAMP (Betz and Fox, 1991; Gold *et al.*, 1994; Hilkens *et al.*, 1995; Okano *et al.*, 2006). However, other reports indicate a pro-inflammatory role for PGE_2. PGE_2 can induce production of IL-23 from dendritic cells (DCs), which promotes the differentiation of pro-inflammatory Th17 cells (Sheibanie *et al.*, 2004; Khayrullina *et al.*, 2008). Recent reports also suggest that PGE_2 can synergize with IL-23 to promote expansion of human Th17 cells and enhance IL-17 production (Chizzolini *et al.*, 2008; Boniface *et al.*, 2009; Napolitani *et al.*, 2009). Furthermore, PGE_2 has been shown to exacerbate symptoms in mouse models of arthritis (Sheibanie *et al.*, 2007a) and inflammatory bowel disease (Sheibanie *et al.*, 2007b), and the blockade of EP_2 and EP_4 receptor signalling in a mouse model of arthritis can alleviate the severity of the disease (Mccoy *et al.*, 2002; Honda *et al.*, 2006).

Here, we show that PGE_2 stimulation of the EP_4 receptor can promote Th1 differentiation, IL-23 production in DCs, and Th17 cell expansion. These effects can be suppressed by a novel EP_4 receptor antagonist ER-819762 ((S)-1'-(3,5-dimethylbenzyl)-2-ethyl-7,9-dimethoxy-10-methyl-5,10-dihydrospiro[benzo[e]imidazo[1,5-a]azepine-1,4'-piperidin]-3(2H)-one) (Spyvee *et al.*, 2009) or an anti-PGE_2 antibody. We also show that oral administration of ER-819762 to DBA/1 mice can effectively suppress disease in collagen-induced arthritis (CIA) or glucose-6-phosphate isomerase (GPI)-induced arthritis models. ER-819762 was also effective in treating chronic inflammatory pain in a rat model. These results suggest that PGE_2 signalling via the EP_4 receptor exerts a pro-inflammatory effect *in vivo* and is physiologically relevant to the pathology of inflammatory arthritis. EP_4 receptors might therefore be an attractive drug target for the treatment of RA, with the potential not only to relieve pain and symptoms but also to modify the underlying aetiology of the disease

Methods

Animals

All animal studies were performed with the approval of the Animal Ethics Committee at Eisai according to Laboratory Animal Welfare guidelines. BALB/c and DO11.10 mice were purchased from Jackson Laboratory. C57BL/6 and DBA/1 mice and F344 rats were purchased from Charles River Laboratories. Mice and rats for each strain were group-housed under controlled conditions with a constant temperature (23 ± 3°C) and humidity (55 ± 5%), a 12-h light/dark cycle and *ad libitum* access to water and standard pelleted food.

Radioligand EP_4 receptor binding assay

The radioligand EP_4 receptor binding assay was performed using ChemiScreen recombinant human EP_4 receptor membrane preparations from Millipore, according to the manufacturer's instructions. Briefly, membranes prepared from Chem-1 cells overexpressing human EP_4 receptor cDNA (Millipore) were mixed with 1.8 nmol·L^{-1} [^{3}H]-PGE_2 and 5 μmol·L^{-1} unlabelled PGE_2 in the presence or absence of various concentrations of ER-819762 in binding buffer [50 mmol·L^{-1} HEPES, pH 7.4, 5 mmol·L^{-1} $MgCl_2$, 1 mmol·L^{-1} $CaCl_2$, 0.2% bovine serum albumin (BSA)] in a nonbinding 96-well plate, and incubated for 1–2 h at room temperature. Prior to filtration, a GF/C 96-well filter plate was coated with 0.33% polyethyleneimine for 30 min, then washed with 50 mmol·L^{-1} HEPES, pH 7.4, 0.5% BSA. Binding reactions were transferred to the filter plate, and washed three times with wash buffer (1 mL per well per wash). The plate was dried and radioactivity counted. Binding of ER-819762 to other related prostanoid receptors was performed by MDS Pharma Services (Bothell, WA, USA) using a similar radiolabelled ligand displacement method.

Cell-based GPCR assays

SE302 is a clone of the human embryonic kidney 293 (HEK/293) cell line containing a reporter driven by cAMP response elements (CRE) in its promoter, and producing secreted placental-like alkaline phosphatase (PLAP). HEK/293 cells express endogenous EP_4 receptors and show induction of PLAP in response to PGE_2 and EP_4 receptor agonists, but not $EP_{1,\ 2}$ or $_3$ receptor agonists (Supplementary Fig. 2). Cells were maintained in DMEM/F12 (50:50) (MediaTech, Inc., Manassas, VA, USA) supplemented with 10% fetal bovine serum (FBS; Tissue Culture Biologicals) plus penicillin/streptomycin. When used for assays, cells were plated in a 96-well plate at 2 × 10^4 cells/100 μL per well in serum-free assay medium (DMEM/F12 supplemented with 0.1% BSA plus penicillin/

streptomycin) and incubated for 4–6 h. Cells were then stimulated with 3 ng mL^{-1} PGE_2 in the presence or absence of various concentrations of ER-819762 overnight, and PLAP activity was measured by mixing 15 μL of culture supernatants with 75 μL of Lumi-phos (Lumigen, Inc.) and 60 μL of assay buffer containing 8 $mmol \cdot L^{-1}$ $MgSO_4$ in 0.1 $mol \cdot L^{-1}$ carbonate-bicarbonate buffer pH11 in a new 96-well black plate and incubated for 2 h at room temperature. Luminescence was read with an Envision 2102 Multilabel reader. Characterization of compound selectivity was performed by Millipore GPCR Profiler Service, which assays intracellular calcium mobilization in cells expressing individual GPCRs and the promiscuous $G\alpha_{16}$ protein. Endogenous EP_2 receptor activity in U2-OS cells was assayed using the EPIC Resonant Waveguide Biosensor system (Corning).

In vitro *T-cell assays*

Naive $CD4^+$ T cells were purified from spleens of either BALB/c or DO11.10 mice by antibody-coated magnetic beads as described by the manufacturer (Robosep; StemCell Technologies). For BALB/c mice, 1×10^5 $CD4^+$ T cells were cultured for 3–6 days in a 96-well plate in 100 μL complete RPMI medium (CellGro) containing 10% regular FBS under: (i) neutral conditions (1 μg mL^{-1} plate-bound anti-CD3 + 1 μg mL^{-1} soluble anti-CD28 + 10 ng mL^{-1} mouse IL-2), (ii) Th1-promoting conditions (neutral + 5 ng mL^{-1} mouse IL-12 + 10 μg mL^{-1} anti-IL-4 antibody) or (iii) Th2-promoting conditions [neutral + 10 ng mL^{-1} of mouse IL-4 + 10 μg mL^{-1} anti-interferon (IFN)-γ antibody]. In experiments where exogenous PGE_2 or EP_4 receptor agonists were added to the culture, charcoal-stripped FBS (Hyclone) was used, which has reduced amounts of lipids. IFN-γ or IL-4 in culture supernatants were quantified by enzyme-linked immunosorbent assay (ELISA). Cell proliferation was assayed with either Alamar Blue or CellTiter-Glo reagents according to the manufacturers' instructions. For DO11.10 mice, mitomycin C-treated splenocytes from BALB/c mice were used as antigen-presenting cells and co-cultured with naive $CD4^+$ T cells in a 5:1 ratio (5×10^5 mitomycin C-treated splenocytes in 100 μL medium + 1×10^5 CD4 T cells in 100 μL medium). These cultures were stimulated with an ovalbumin peptide 323-339 (OVA peptide; 0.3 ng mL^{-1}) under neutral, Th1- or Th2-promoting conditions, as described above. EP_4 receptor agonists and antagonists, other cAMP-inducing agents, inhibitors of PI3K or protein kinase A (PKA) or anti-PGE_2 antibody were added during Th cell differentiation.

In order to study the effect of EP_4 receptor agonists, antagonists and cAMP-inducing agents on IL-17 production, total $CD4^+$ T cells isolated from spleens of C57BL/6 mice were activated with plate-bound anti-CD3 (2 μg mL^{-1}) plus soluble anti-CD28 (2 μg mL^{-1}) in the presence or absence of IL-23 (10 ng mL^{-1}) and presence or absence of EP_4 receptor agonist/antagonists or other agents at the indicated concentrations for 3–5 days. Culture supernatants were analysed by IL-17 ELISA, and cell proliferation was measured with CellTiter-Glo.

IL-23-induced Th17 expansion

$CD4^+$ T cells were isolated from C57BL/6 mice and activated with antibody against T cell receptor β chain (1 μg mL^{-1} plate-bound) and anti-CD28 (2 μg mL^{-1} soluble) with or without IL-23 (30 ng mL^{-1}) for 5 days in complete RPMI medium containing 10% normal FBS. IL-17-producing cells were analysed by IL-17 intracellular staining. Briefly, cells were stimulated for 5 h with phorbol 12-myristate 13-acetate (50 ng mL^{-1}), ionomycin (500 ng mL^{-1}) and Golgistop (1 μL mL^{-1}), stained with anti-CD4 antibody, fixed and permeabilized (Cytofix/Cytoperm) and stained with anti-IL-17 antibody (all from BD Biosciences) and then analysed by flow cytometry.

In vitro *human monocytes-derived DC assay*

Human peripheral blood monocytes (PBMC) were isolated by Ficoll gradient from heparinized venous blood of healthy, drug-free volunteers, following written informed consent. $CD14^+$ cells were purified from human PBMC using Miltenyi CD14 microbeads according to the manufacturer's instructions, and differentiated with human GM-CSF (500 U mL^{-1}) + human IL-4 (500 U mL^{-1}) in complete RPMI medium containing 10% charcoal-stripped FBS for 8 days. Detached immature DCs (imDCs) were stimulated with lipopolysaccharide (LPS) (*Escherichia coli* 0111:B4; 10 ng mL^{-1}) and the Toll-like receptor (TLR)7 ligand, R-848 (2.5 μg mL^{-1}) with or without the addition of EP_4 receptor agonist/antagonists or anti-PGE_2 at the concentrations indicated for 24 h. Concentrations of IL-23 in culture supernatants were measured by ELISA (eBioscience).

Collagen-induced arthritis model

Male DBA/1 mice were immunized by injection at the base of the tail with 0.1 mL emulsion containing 150 μg bovine type II collagen (bCII) emulsified in complete Freund's adjuvant (CFA). Three weeks after the first immunization, all mice were boosted with bCII emulsified in Freund's incomplete adjuvant. ER-819762 was given orally daily at a dose of 10, 30 or 100 $mg \cdot kg^{-1}$ from day 20 after primary immunization but before disease onset (prophylactic evaluation) or after the disease induction (therapeutic evaluation). The severity of arthritic symptoms in the paws of each mouse was graded, in a double-blind manner, according to Williams (2004). At the end of the experiments, knee and ankle joints were used for radiography analysis. X-ray score was defined as the total score of a combination of osteopenia, bone erosion and new bone formation as follows: 0 – no change; 1 – slight change, 2 – moderate change; 3 – severe change (Kop *et al.*, 2006). Each treatment group consists of six to eight mice.

GPI-induced arthritis model

Male DBA/1 mice were immunized by injecting at the base of the tail 0.15 mL of emulsion containing 300 μg recombinant human GPI-glutathione-S-transferase fusion protein (hGPI) in CFA. ER-819762 was given orally daily at a dose of 10 or 30 $mg \cdot kg^{-1}$ from day 6 after primary immunization but before disease onset (prophylactic evaluation) or after the disease induction (therapeutic evaluation). Each treatment group consisted of six to eight mice. Arthritic animals were clinically assessed by an arthritis scoring system as follow (Iwanami *et al.*, 2008): 0 = no evidence of inflammation, 1 = subtle

inflammation or localized oedema, 2 = easily identified swelling but localized to dorsal or ventral surface of paws, and score 3 = swelling on all aspects of paws. Serum samples were collected at the end of the study and analysed for cytokine levels by ELISA. To analyse popliteal lymph node cells, emulsified GPI was injected into the foot pad of DBA/1 mice and ER-819762 was orally administered once daily at 30 mg·kg^{-1} from the day of immunization. Lymph nodes were removed 6 days later, and cells were stimulated with 10 μg mL^{-1} recombinant GPI and GolgiStop (BD) for 12 h (Iwanami *et al.*, 2008). IL-17- and IFN-γ-producing cells were analysed as described above.

CFA-induced hyperalgesia

Complete Freund's adjuvant, consisting of 100 μg of *Mycobacterium tuberculosis* H37 RA (Difco, Detroit, MI, USA) in 100 μL of liquid paraffin (Wako Pure Chemicals), was injected into the right hind footpad of 7-week-old male F344 rats. Three days after CFA injection, rats exhibited a lame walking reaction consisting of a three-legged gait. ER-819762 or indomethacin was orally administered at day 3 and the inhibitory effect on the lame walking reaction was evaluated, without knowledge of treatment, after 2–3 h of dosing (Higuchi *et al.*, 1986). Each treatment group consisted of seven rats.

Ex vivo lymph node studies

Male DBA/1 mice were immunized with bCII emulsified in CFA, as described above. ER-819762 was orally administered daily at a dose of 30 mg·kg^{-1} from the day of immunization. Suspensions of single cells were prepared from draining lymph nodes from mice, 15 days after immunization. Cells were plated in a 96-well plate at 4 × 10^5 cells per 200 μL per well in complete RPMI medium and stimulated with either bCII (50 μg mL^{-1}) or phosphate-buffered saline for 72 h. Cytokine production in culture supernatants was analysed by ELISA, and cell proliferation was measured by CellTiter-Glo.

Data analyses

All values shown in the text and figures are mean ± SD. Nonlinear regression analysis of the data and calculation of IC_{50} values were performed using Prism 4 (GraphPad Software, San Diego, CA, USA). Statistical analysis was performed by Dunnett-type multiple comparison test or paired *t*-test; a value of $P < 0.05$ (two-sided) was considered statistically significant.

Materials

ER-819762 ((S)-1′-(3,5-dimethylbenzyl)-2-ethyl-7,9-dimethoxy -10-methyl-5,10-dihydrospiro [benzo[e]imidazo [1,5-a]azepine-1,4′-piperidin]-3(2H)-one) was synthesized at Eisai Research Institute of Boston Inc. Indomethacin was purchased from Cayman Chemicals. For *in vitro* testing, ER-819762 was dissolved in 100% dimethyl sulphoxide (DMSO) and the final concentration of DMSO in the assay was 0.1%. For *in vivo* evaluation, ER-819762 or indomethacin was suspended in 0.5% (w/v) methylcellulose and orally administered at 10 mL·kg^{-1} per mouse or 5 mL·kg^{-1} per rat.

Mouse IL-2, IL-12, IL-23 and human GM-CSF were purchased from R&D Systems. Human IL-4 and GM-CSF were from Peprotec. Anti-CD3 (clone 145-2C11), anti-CD28 (clone 37.51), anti-IL-4 (clone 11B11), anti-IFN-γ (clone XMG12) and PE-anti-mouse IL-17 (clone TC11-18H10) were purchased from BD Pharmingen. Anti-TCR (clone H57-597) was purchased from eBioscience. OVA peptide, mitomycin C, H-89, KT5721, LY-294002 and isobutylmethylxanthine (IBMX) were purchased from Sigma. PGE_2, PGE_1-alcohol (PGE_1–OH), butaprost, forskolin and anti-PGE_2 IgG1 monoclonal antibody (clone 2B5) were purchased from Cayman Chemicals. LPS and R-848 were from InVivoGen. CD14$^+$ cell isolation kits were from MiltenyiBiotec. CD4$^+$ T cell isolation kits were from MiltenyiBiotec or StemCell Technologies. IFN-γ ELISA kits were from Pierce; IL-4 ELISA kits are from R&D Systems; IL-23 ELISA kits were from eBioscience. Intracellular IL-17 staining reagents were from BD Biosciences. Alamar Blue reagents were from Biosource International. CellTiter-Glo reagents were from Promega. CFA for mouse RA models was an emulsion form prepared by Difco (Michigan) and CFA for the lame walking model was desiccated powder from Difco, which we suspended in liquid paraffin (Wako Chemicals).

Results

Identification of selective EP_4 receptor antagonists

In the course of screening for drugs unrelated to the prostanoid receptors, we discovered a series of compounds that could suppress the expression of a stably transfected cytomegalovirus (CMV) promoter in HEK/293 cells. The CMV promoter is known to be modulated by cAMP signalling (Hunninghake *et al.*, 1989), and we found that these compounds inhibited the induction of CMV promoter activity by a factor present in FBS. The inducing factor in FBS was identified as PGE_2 and induction of cAMP was found to be mediated solely by the endogenous EP_4 receptor in HEK/293 cells (Supplementary Figs 1 and 2). A representative of this series of compounds, ER-819762 (structure shown in Fig. 1D), displaced PGE_2 binding to human EP_4 receptors (IC_{50} value of 70 ± 11 nmol·L^{-1}; Fig. 1A), but did not displace ligand binding to several related human prostanoid GPCRs, including EP_2, DP, CRTH2 and TP receptors, and the leukotriene GPCRs LTB_4, $CysLT_1$ and $CysLT_2$ receptors (Fig. 1C). ER-819762 also suppressed human EP_4 receptor-mediated cell signalling as measured in a cAMP-dependent reporter assay (IC_{50} value of 59 ± 6 nmol·L^{-1}) (Fig. 1B). In a larger cell signalling panel of 107 GPCRs, ER-819762 (1 μmol·L^{-1}) was highly selective for EP_4 receptors, exhibiting no agonism or antagonism for any other receptor, including the related PGE_2 EP_1, EP_2 and EP_3 receptors (Table 1).

EP_4 receptor antagonism suppresses in vitro *Th1 differentiation*

As PGE_2 has been reported to modulate T cell differentiation and function, we tested the effect of ER-819762 in Th1 and Th2 differentiation assays. Th1 differentiation was induced by activating naïve CD4$^+$ T cells with anti-CD3 and anti-CD28 antibodies in 10% charcoal-stripped FBS in the presence of

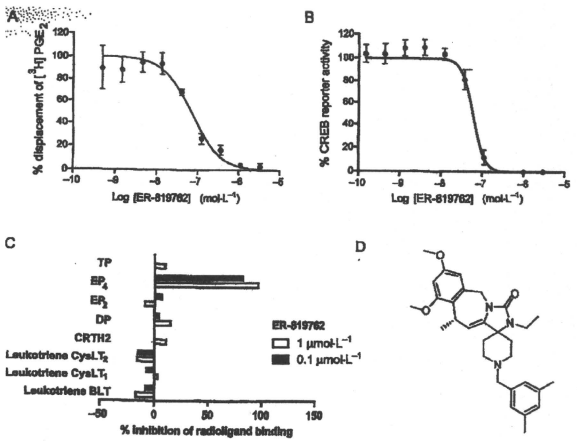

Figure 1 Activity and structure of ER-819762. (A) Competitive displacement of radiolabelled prostaglandin E_2 (PGE_2) from cell membranes overexpressing EP_4 receptors (Millipore ChemiScreen). (B) Inhibition of PGE_2-induced cAMP response element–placental-like alkaline phosphatase reporter activity in human embryonic kidney cells, which express endogenous EP_4 receptors (Supplementary Figure 2). Data are representative of mean ± SD derived from three independent experiments. (C) Competitive displacement of radiolabelled ligands from cell membranes overexpressing various prostanoid and leukotriene receptors by 0.1 and 1 μmol·L^{-1} ER-819762 (data from MDS Pharma, Bothel, WA, USA). (D) Chemical structure of ER-819762: (S)-1'-(3,5-dimethylbenzyl)-2-ethyl-7,9-dimethoxy-10-methyl-5,10 dihydrospiro[benzo[e]imidazo[1,5-a]azepine-1,4'-piperidin]-3(2H)-one.

IL-2, IL-12 and anti-IL-4 antibody. Th2 differentiation was induced by IL-4 and anti-IFN-γ antibody. Addition of PGE_2, butaprost (an EP_2 receptor agonist) and prostaglandin E_1 alcohol (PGE_1-OH; an EP_3/EP_4 receptor agonist) significantly enhanced the differentiation of naïve CD4$^+$ T cells into Th1 cells (Fig. 2A). ER-819762 suppressed PGE_2- and PGE_1-OH-induced IFN-γ production by Th1-differentiating cells in a concentration-dependent manner (Fig. 2B), but had no effect on cellular ATP levels (CellTiter-Glo, Promega), an indicator of cell metabolic activity. Figure 2B also shows that ER-819762 inhibited IFN-γ in the absence of added prostaglandins, suggesting that the PGE_2 produced by the T cells themselves acts in an autocrine manner to promote Th1 differentiation. ER-819762 had no effect on butaprost-stimulated IFN-γ production at up to 1 μmol·L^{-1} (Supplementary Fig. 3). Th1 and Th2 differentiation were also induced by co-culturing naïve CD4$^+$ T cells isolated from DO11.10 mice with mitomycin C-treated splenocytes and activating with the OVA peptide under neutral, Th1- or Th2-polarizing conditions in normal 10% FBS as described in *Methods*. In this experiment, IFN-γ production was suppressed by either ER-819762 or a neutralizing monoclonal anti-PGE_2 antibody (clone 2B5; Fig. 2C), and these effects were non-additive. We also observed no effect of ER-819762 on Th2 differentiation at up to 10 μmol·L^{-1} (Fig. 2D).

Although Th1 differentiation was enhanced by PGE_2, as measured by increased IFN-γ production (Fig. 2), neither forskolin, an activator of adenylate cyclase, nor IBMX, a phosphodiesterase inhibitor, caused a statistically significant enhancement in IFN-γ production (Fig. 3A), suggesting that the promotion of Th1 differentiation by PGE_2 was not due to cAMP signalling. Moreover, PGE_2-stimulated Th1 differentiation was not suppressed by the PKA inhibitors H-89 (1 μmol·L^{-1}) or was only weakly suppressed by a structurally unrelated PKA inhibitor KT-5720 (10 μmol·L^{-1}), but was strongly suppressed by the PI3K inhibitor LY294002 (2 μmol·L^{-1}), as well as by ER-819762 (Fig. 3B). Higher concentrations of H-89 (10 μmol·L^{-1}) were toxic (data not shown). These results suggest that the PI3K pathway, but not the PKA-cAMP signalling pathway functioning downstream of EP_4 receptors is primarily responsible for PGE_2-enhanced Th1 differentiation. Butaprost also induced Th1 differentiation (Fig. 2A), raising the possibility that EP_2 receptors may signal via PI3K in addition to PKA-cAMP.

EP_4 receptor antagonism suppresses IL-23 secretion in human monocyte-derived DCs

It was recently reported that PGE_2 can promote Th17 cell differentiation in mice by inducing DCs to preferentially produce IL-23 (Sheibanie *et al.*, 2007a; Khayrullina *et al.*, 2008). Similarly, receptors that mobilize cAMP have been reported to enhance IL-23 secretion by human DCs (Schnurr *et al.*, 2005). We therefore examined the role of EP_4 receptor signalling in immature human dendritic cells (imDCs). imDCs were generated from CD14$^+$ monocytes by differentiation with GM-CSF plus IL-4 and assayed for IL-23 production in media containing charcoal-stripped FBS. IL-23 production

Table 1 Selectivity of ER-819762 against 107 G protein-coupled receptors (GPCRs)

GPCR Target	% inhibition by ER-819762 (1 μmol·L⁻¹)	GPCR Target	% inhibition by ER-819762 (1 μmol·L⁻¹)	GPCR Target	% inhibition by ER-819762 (1 μmol·L⁻¹)
M1 (CHRM1)	1.1% ± 1.9%	CCK2 (CCKBR)	−8.1% ± 4.0%	NTR1	−3.7% ± 1.1%
M2 (CHRM2)	−10.5% ± 0.8%	CRF1 (CRHR1)	−16.2% ± 0.4%	FPR1	−6.6% ± 1.1%
M3 (CHRM3)	−3.2% ± 0.4%	CRF2 (CRHR2)	−9.5% ± 0.1%	FPR2/FPRL1	−7.3% ± 1.9%
M5 (CHRM5)	−4.7% ± 4.0%	D1	−8.1% ± 1.5%	NOP/ORL1	−11.2% ± 2.4%
A1 (ADORA1)	4.9% ± 6.0%	D2	0.6% ± 6.6%	δ (OPRD1)	−11.3% ± 1.0%
A3 (ADORA3)	−0.8% ± 1.4%	D5	25.2% ± 9.5%	κ (OPRK1)	8.3% ± 11.7%
A2A (ADORA2A)	13.4% ± 4.5%	ETA (EDNRA)	4.2% ± 2.4%	OX2 (HCRTR2)	−1.3% ± 0.3%
A2B (ADORA2B)	−1.4% ± 4.2%	GPR40	−3.1% ± 3.1%	PTH1 (PTHR1)	−4.7% ± 5.3%
α1A (ADRA1A)	−2.2% ± 0.1%	GPR43	5.1% ± 2.5%	PAF (PTAFR)	1.6% ± 2.3%
α2A (ADRA2A)	−13.2% ± 5.7%	GABBAb1	−9.7% ± 0.5%	PK1/GPR73	−0.4% ± 5.3%
β1 (ADRB1)	−12.1% ± 3.9%	GAL1 (GALR1)	22.9% ± 1.9%	PRP/GPR10	6.7% ± 0.7%
β2 (ADRB2)	−4.2% ± 3.4%	GCGR	−4.5% ± 2.0%	PTGDR (DP)	−13.7% ± 1.8%
C3aR	8.5% ± 0.3%	mGlu1	0.6% ± 8.2%	PTGER1 (EP1)	−4.6% ± 0.1%
C5aR	−10.2% ± 0.1%	GnRH	−12.3% ± 1.1%	PTGER2 (EP2)	(See legend)
ChemR23	3.5% ± 2.4%	H1 (HRH1)	−4.6% ± 1.0%	PTGER3 (EP3)	−2.4% ± 0.0%
AT1	−2.7% ± 1.7%	H2 (HRH2)	−4.8% ± 0.9%	PTGFR (FP)	0.1% ± 5.1%
BB2 (GRPR)	8.1% ± 0.3%	NK1 (TACR1)	−7.7% ± 6.2%	**PTGER4 (EP4)**	**90.3% ± 0.7%**
BB1	5.2% ± 4.6%	NK2	0.3% ± 2.6%	PTGIR (IP)	(See legend)
B2 (BDKRB2)	5.7% ± 1.3%	H3 (HRH3)	2.9% ± 4.1%	TBXAR2 (TP)	−9.8% ± 5.1%
AMY1	12.0% ± 0.9%	GPRS4	−11.2% ± 4.4%	PAR1	−5.1% ± 9.3%
CGRP1	−7.6% ± 8.0%	BLT1 (LTB4R1)	−3.3% ± 2.9%	PAR2	−6.1% ± 8.0%
CaS	−12.6% ± 0.2%	CysLT1	−4.4% ± 4.0%	5–HT1A (HTR1A)	0.9% ± 4.5%
CB1	0.0% ± 2.5%	CysLT2	−0.7% ± 3.9%	5–HT1B	6.9% ± 15.6%
CXCR1	−5.1% ± 3.0%	S1P2 (EDG5)	−16.2% ± 0.9%	5–HT2B (HTR2B)	2.2% ± 2.9%
CXCR2	−1.7% ± 2.5%	S1P3 (EDG3)	−5.9% ± 0.6%	5–HT2C (HTR2C)	11.4% ± 3.8%
CXCR3	−14.6% ± 7.8%	LPA1 (EDG2)	−11.9% ± 5.9%	SST3	−8.9% ± 11.3%
CXCR4	−6.1% ± 2.4%	LPA3 (EDG7)	−0.2% ± 1.0%	SST4	−12.4% ± 1.8%
CCR1	−3.5% ± 1.2%	MRGX2	−8.6% ± 1.3%	GPR68(OGR1)	0.0% ± 0.0%
CCR2b	−6.7% ± 4.7%	MCHR1	−0.2% ± 0.5%	TRH	−6.9% ± 2.9%
CCR4	−10.6% ± 5.8%	MCHR2	−10.2% ± 4.0%	V1A	−0.6% ± 1.0%
CCR6	−7.5% ± 4.5%	MC4R	−3.6% ± 10.5%	V1B (AVPR1B)	−5.0% ± 1.5%
CCR7	9.6% ± 5.5%	Motilin	−12.6% ± 3.3%	V2 (AVPR2)	−17.8% ± 0.2%
CCR8	−13.2% ± 16.2%	NMUR1	−12.2% ± 4.6%	OT (OXTR)	6.5% ± 9.0%
CCR9	−15.1% ± 0.4%	Y1 (NPY1R)	15.8% ± 7.0%	PAC1 long	−7.5% ± 2.3%
CCR10	6.0% ± 2.5%	Y2 (NPY2R)	−17.7% ± 1.9%	VPAC1 (VIPR1)	−10.5% ± 1.0%
CRTH2	−2.8% ± 3.5%			VPAC2 (VIPR2)	−12.0% ± 1.9%

ER-819762 was assayed by Millipore GPCR Profiler Service, which monitors calcium flux in cells expressing the specific GPCR and promiscuous GPCR-coupling $G\alpha_{15/16}$ proteins. Both agonism and antagonism of the GPCRs listed above were examined, except for EP_2 and IP receptors. No significant agonism (>15%) was found for any GPCR (data not shown), and only antagonism of EP_4 receptors was found. ER-819762 was not able to displace binding of radiolabelled PGE_2 to EP_2 receptors (Fig. 1C, MDS Pharma Profiling Service. We also used the human U2-OS cell line, which endogenously expresses EP_2 and IP but not EP_4 receptors, to assay agonism and antagonism by ER-819762 using the Corning EPIC Resonate Waveguide Biosensor system. We observed no antagonism of butaprost- (EP_2 receptors) or iloprost- (IP receptors) induced signalling by 10 μM ER-819762, and no signalling induced by compound alone in this cell line (data not shown). Bold texts indicate positive results.

could be induced in imDCs by stimulation with LPS, a ligand for the TLR4, and co-stimulation with the TLR7 ligand R-848 (Fig. 4A), but not by LPS or R-848 alone (data not shown). We found that the $EP_3/_4$ receptor agonist PGE_1-OH enhanced LPS/R-848-induced IL-23 production in imDCs and that this response was antagonized by ER-819762 (Fig. 4A). These experiments were performed using charcoal-stripped 10% FBS, yet we observed that IL-23 production was partially suppressed by either ER-819762 (Fig. 4A) or by anti-PGE_2 antibody (Fig. 4B) in the absence of added prostaglandins. This suggests that IL-23 production in these activated DCs involves endogenously produced PGE_2.

EP_4 receptors antagonism suppresses IL-17 production and inhibits IL-23-induced Th17 expansion in activated $CD4^+$ T cells in vitro

We next determined whether EP_4 receptor stimulation might influence the development or function of Th17 cells, which play a critical role in inflammation and autoimmune diseases (Fouser *et al.*, 2008). First we tested the effect of EP_4 receptor stimulation on IL-17 production, a typical cytokine of Th17 cells, in activated $CD4^+$ T cells. Total $CD4^+$ T cells were isolated from mouse splenocytes, which include both naïve and memory T cells, and pre-existing Th17 cells were stimulated for 3–5 days using IL-23 and either anti-TCRβ or anti-CD3/anti-CD28 antibodies. Addition of PGE_2, butaprost or PGE_1-OH (Fig. 5A) suppressed overall T cell proliferation, yet enhanced IL-17 production. Both of these PGE_2-induced effects were reversed by 0.1 or 1.0 $\mu mol \cdot L^{-1}$ ER-819762 (Fig. 5B). Further analysis by flow cytometry showed that PGE_2 stimulation increased the percentage of IL-17-producing cells within this population (Fig. 5C), and that this increase was suppressed by ER-819762 (data not shown). ER-819762 (Fig. 5D) or anti-PGE_2 antibody (Supplementary Fig. 4) could also suppress IL-23-induced Th17 expansion in the absence of exogenously added PGE_2. However, some PGE_2 could be present in the media, because we used normal 10% FBS and